HHMI Author Manuscript

HHMI Author Manuscript

HHMI Author Manuscript

PubMed Central

HHMI
HOWARD HUGHES MEDICAL INSTITUTE

AUTHOR MANUSCRIPT
Accepted for publication in a peer-reviewed journal

Published as: *Neuron*. 2009 July 30; 63(2): 203–215.

Tweek, an evolutionary conserved proteinis required for synaptic vesicle recycling

Patrik Verstreken[1,4,5,*], **Tomoko Ohyama**[1,*], **Claire Haueter**[1], **Ron L.P. Habets**[4,5], **Yong Q. Lin**[1], **Laura E. Swan**[6], **Cindy V. Ly**[2], **Koen J. T. Venken**[1,3], **Pietro De Camilli**[6], and **Hugo J. Bellen**[1,2,3,§]

[1]Department of Molecular and Human Genetics and Howard Hughes Medical Institute, Baylor College of Medicine, One Baylor Plaza, Houston, TX, USA

[2]Department of Neuroscience, Baylor College of Medicine, One Baylor Plaza, Houston, TX, USA

[3]Program in Developmental Biology, Baylor College of Medicine, One Baylor Plaza, Houston, TX, USA

[4]VIB, Department of Molecular and Developmental Genetics, Program in Molecular and Developmental Genetics, Program in Cognitive and Molecular Neuroscience, Laboratory of Neuronal Communication, Herestraat 49, Leuven, Belgium

[5]K.U.Leuven, Center for Human Genetics, Program in Molecular and Developmental Genetics, Program in Cognitive and Molecular Neuroscience, Laboratory of Neuronal Communication, Herestraat 49 Leuven, Belgium

[6]Department of Cell Biology, Howard Hughes Medical Institute, Kavli Institute for Neuroscience, Yale University School of Medicine, New Haven, CT, USA

Abstract

Synaptic vesicle endocytosis is critical to maintain synaptic communication during intense stimulation. Here we describe Tweek, a conserved protein that is required for synaptic vesicle recycling. *tweek* mutants show reduced FM 1–43 uptake, cannot maintain release during intense stimulation and harbor larger than normal synaptic vesicles, implicating it in vesicle recycling at the synapse. Interestingly, the levels of a fluorescent $PI(4,5)P_2$ reporter are reduced at *tweek* mutant synapses and the probe is aberrantly localized during stimulation. In addition, various endocytic adaptors known to bind $PI(4,5)P_2$ are mislocalized and the defects in FM 1–43 dye uptake and adaptor localization are partially suppressed by removing one copy of the phosphoinositide-phosphatase *synaptojanin*, suggesting a role for Tweek in maintaining proper phosphoinositide levels at synapses. Our data implicate Tweek in regulating synaptic vesicle recycling via an action mediated at least in part by the regulation of $PI(4,5)P_2$ levels or availability at the synapse.

© 2009 Elsevier Inc. All rights reserved.

§Correspondence: hbellen@bcm.tmc.edu.
*Equal contribution

Publisher's Disclaimer: This is a PDF file of an unedited manuscript that has been accepted for publication. As a service to our customers we are providing this early version of the manuscript. The manuscript will undergo copyediting, typesetting, and review of the resulting proof before it is published in its final citable form. Please note that during the production process errors may be discovered which could affect the content, and all legal disclaimers that apply to the journal pertain.

HHMI Author Manuscript
HHMI Author Manuscript
HHMI Author Manuscript

Introduction

Synaptic vesicle recycling relies heavily on clathrin dependent endocytosis, ensuring a continuous supply of new synaptic vesicles during stimulation (Haucke, 2003; Kasprowicz et al., 2008). Numerous proteins involved in the process have been identified through biochemical screening approaches and forward genetic screens in model organisms (Babcock et al., 2003; Jung and Haucke, 2007). Several protein adaptors and lipids coordinately bind and recruit downstream effectors that mediate membrane bending to shape new vesicles. The coordinated action of dynamin and its effectors results in separation of new vesicles that are subsequently prepared for a new round of fusion (van der Bliek and Meyerowitz, 1991). While numerous proteins and lipids have been assigned a specific function during this process, others play a supporting role to scaffold synaptic zones, ensuring a high fidelity of recycling (Koh et al., 2004; Majumdar et al., 2006).

Phosphoinositide lipids (PIs) play important regulatory roles in various cellular processes, including vesicle recycling (Martin, 1998; Vicinanza et al., 2008). PI(4,5)P_2 is concentrated at the plasma membrane of most cells, including neurons, and plays multiple roles in the regulation of synaptic transmission (Cremona et al., 1999; Di Paolo et al., 2004; Harris et al., 2000; Micheva et al., 2001; Van Epps et al., 2004; Verstreken et al., 2003). PI(4,5)P_2 is a precursor for the phospholipase C-derived metabolites, IP_3 and DAG, which are involved in the regulation of Ca^{2+} release from intracellular stores and vesicle priming and fusion, respectively (Davis and Patrick, 1990; Rhee et al., 2002; Sladeczek, 1987). PI(4,5)P_2 also appears to regulate the size of the readily releasable pool of synaptic vesicles and secretory granules (Di Paolo et al., 2004; Gong et al., 2005; Milosevic et al., 2005). In addition, PI(4,5)P_2 is implicated in the formation of new synaptic vesicles at the plasma membrane (Cremona et al., 1999; Harris et al., 2000; Mani et al., 2007; Van Epps et al., 2004; Verstreken et al., 2003). Hence, at the synapse, altered levels of PI(4,5)P_2 may affect several steps in the synaptic vesicle cycle. However, despite these pleiotropic functions, PI metabolism within the cell is surprisingly spatially restricted and PI-dependent processes appear to be locally regulated (Di Paolo et al., 2002; Golub and Caroni, 2005; Schuske et al., 2003).

Here we report the identification and characterization of a Tweek, a conserved and previously uncharacterized protein. Tweek is required to maintain normal synaptic vesicle recycling and affects PI availability. Our data suggest that Tweek may regulate synaptic vesicle recycling, at least in part, by affecting PI(4,5)P_2 pools at the synapse.

Results

Isolation of *tweek* mutants

To identify proteins that affect synaptic transmission and plasticity, we performed genetic screens using *ey-FLP* technology (Newsome et al., 2000; Stowers and Schwarz, 1999; Verstreken et al., 2003). These screens allow us to identify flies that carry random chemically induced (EMS) mutations that affect synaptic transmission in photoreceptors, circumventing the organismal lethality associated with these mutations. Flies with mutant eyes were screened by recording electroretinograms (ERG) (Figure 1A). ERGs measure differences in extracellular potential between photoreceptors (PRs) and the body during a short light flash (1 s). In controls, ERG recordings show (1) a de- and repolarization of the PRs, reflecting an intact phototransduction mechanism, and (2) ‘on’ and ‘off’ transients at the onset and conclusion of the light pulse, indicating that the PRs can activate postsynaptic neurons (Figure 1A, grey arrowheads). By isolating mutants with defective on and off transients but normal depolarization, we and others have been able to identify genes that affect synaptic function or development (Babcock et al., 2003; Verstreken et al., 2003). Two mutations in one of the complementation groups on chromosome arm 2L, *tweek*, show ‘on’ and ‘off’ transient

HHMI Author Manuscript HHMI Author Manuscript HHMI Author Manuscript

amplitudes that are severely reduced compared to controls (Figure 1A). These data suggest that *tweek* mutant PRs fail to properly transmit information to post-synaptic neurons.

To better understand the underlying cause of the defect in neuronal communication in *tweek* mutant eyes, we performed transmission electron microscopy (TEM), revealing ultrastructural features of the mutant PR synapses, including mitochondrial density and morphology, active zone integrity, glial cell morphology, and synaptic vesicle density. PRs invade the lamina, the first optic neuropil of the fly brain, cluster in groups of six and form characteristic topographic connections on post synaptic cells. One such unit, containing six PRs, labeled green in Figure 1B–C, is a lamina cartridge. Qualitative analyses indicate that most synaptic components are normal in *tweek* mutant PR terminals (Figure 1B–E), however synaptic vesicle density appears markedly reduced (Figure 1D–E). In addition, although the number of glial invaginations in the PR cells (capitate projections) is not different between controls and mutants (controls: 0.355 ±0.026 capitates μm^{-1}; $tweek^{1}$: 0.352±0.041 μm^{-1}; $p<0.01$), capitate projections are not deeply invaginated or headed in the mutants but often remain shallow (controls: 17.9±4.1% shallow projections and $tweek^{1}$: 68.3±13.9% shallow projections; $p<0.01$; Figure 1D, E). Since glial invaginations are thought to be sites of endocytosis in PR terminals (Fabian-Fine et al., 2003), these data, together with the lower vesicle density, suggest that while development of the PR terminals is not much impaired, mutations in *tweek* may affect synaptic function, possibly endocytosis.

tweek mutants further sparked our interest as rare homozygous flies survive to adulthood. These flies are unable to walk or stand upright for long periods, and exhibit seizures, suggestive of severe neurological defects. Based on the adult behavior of the mutants we named the gene "*tweek*" as it reminded us of the cartoon character "Tweek" from the TV series "Southpark". However, even when grown under optimal conditions (see Methods) most homozygous $tweek^{2}$ or trans-heterozygous $tweek^{1}/Df$ and $tweek^{2}/Df$ mutants die as late pupae and only very few animals eclose (<1/2,000) and die soon after eclosion. Hence, *tweek* is an essential gene.

tweek encodes a large protein of unknown domain structure

To identify the gene encoding *tweek*, we mapped the lesions in the mutants using meiotic recombination (Zhai et al., 2003). Rough mapping placed *tweek* in the 36A–C cytological interval and showed that the mutations fail to complement *Df(2L)Exel8036* (Parks et al., 2004). Meiotic fine-mapping (Figure 2A), allowed us to map the lesions in the *tweek* alleles between *EY12630* and *KG05250*.

To confirm the mapping position we crossed the *tweek* EMS alleles to flies that carry lethal transposon insertions in the region. The PiggyBac insertion *c01084* (Parks et al., 2004) located downstream of the start codon in *CG15133* as well as the *P*-element insertion *EY02585* (Bellen et al., 2004) located between *ApepP* and *CG4841* and an imprecise excision of this *P*-element ($EY02585^{\Delta 1}$), removing the start codons of *ApepP* and *CG4841*, all fail to complement the *tweek* alleles and *Df(2L)Exel8036* (Figure 2B,C and E). An excision of the PiggyBac insertion ($c01084^{\Delta}$ in Figure 2E) and a precise excision of the *P* element reverts the lethality and complement the *tweek* alleles and the deficiency. Although *CG15133* and *CG4841* are separated by 4 genes encompassing more than 12 kb, *c01084* and $EY02585^{\Delta 1}$ also fail to complement one another, suggesting that both mutations affect the same gene.

As shown in Figure 2B *CG15134* is the only gene located between *CG15133* and *CG4841* that is transcribed in the same orientation. To determine if *CG15133*, *CG15134* and *CG4841* encode a single gene, we performed RT-PCR experiments using cDNAs prepared from control, $c01084^{\Delta}$, *c01084/Df* and homozygous *c01084* flies. Although we were able to amplify and sequence control and $c01084^{\Delta}$ cDNA fragments using primers in *CG15133* and *CG15134*, primers in *CG15134* and *CG4841* and primers in *CG15133* and *CG4841* (Figure 2C, data not

HHMI Author Manuscript HHMI Author Manuscript HHMI Author Manuscript

shown and supplemental Table 1), no such fragments could be recovered from homozygous *c01084* animals. Hence, our data indicate that *CG15133*, *CG15134* and *CG4841*, can form one transcript. Furthermore, the PiggyBac (*c01084*) insertion in *CG15133* greatly reduces or abolishes expression of these three separately annotated *CGs*, suggesting it is a strong hypomorphic or null allele of *tweek*. Hence, *CG15133*, *CG15134* and *CG4841* are jointly transcribed as a large transcript and this transcript corresponds to *tweek*.

The 5'UTR of *tweek* is not annotated and we therefore performed Rapid Amplification of 5' Complementary DNA Ends (5'RACE). We were able to amplify 108 bp 5' of the ATG start codon in *CG15133*, identifying the 5'UTR of *tweek*. These data also place the *c01084* insertion inside *tweek* and we therefore renamed *c01084* as $tweek^{c01084}$. However, the previously annotated second exon of *CG15133* does not appear amplifiable in our assays and the gene structure based on our RT-PCR and 5'RACE results is shown in Figure 2C.

We also found a 74 bp deletion and a 6 bp insertion leading to a premature stop codon in $tweek^{1}$ and an AG to AA splice acceptor mutation before exon 20 in $tweek^{2}$, predicting a frame shift (Figure 2C). This splice acceptor mutation in $tweek^{2}$ was also confirmed by RT-PCR (Figure S1 and supplemental Table 1). Since $tweek^{c01084}/tweek^{1}$, $tweek^{c01084}/tweek^{2}$, $tweek^{1}/Df(2L)Exel8036$, $tweek^{2}/Df(2L)Exel8036$, $tweek^{c01084}/Df(2L)Exel8036$ and $tweek^{2}/tweek^{2}$ show a similar lethal phase, our data suggest that $tweek^{c01084}$, $tweek^{1}$ and $tweek^{2}$ are all severe hypomorphic alleles or null alleles of *tweek* (Figure 2E). Finally, *tweek* corresponds to *CG15133*, *CG15134*, and *CG4841* as all mutations in trans over a *Df* can be rescued using P (acman) clones (Venken et al., 2006) that contain genomic DNA encompassing *CG4841*, *CG15133* and *CG15134* (Figure 1A, green bar in Figure 2B and supplemental Table 2); however, the *tweek* alleles cannot be rescued with a 21 kb construct encompassing the *CG4841* sequence (red bar in Figure 2B). Based on sequence annotation and RT-PCR data, our data indicate that the *tweek* mRNA transcript is 16,124 bp and the Tweek protein encompasses and ORF of 5,076 amino acids (~565 kDa). Although *tweek* encodes a very large and evolutionary conserved protein, it contains no known protein domains or motifs, including transmembrane domains or nuclear localization signals. Nonetheless, BLAST searches reveal that Tweek has homologues from nematode to man (Figure S2). In most species including various Drosophilids, mosquitoes, and mouse, the three CGs identified as *tweek*, correspond to two or three adjacent transcripts annotated as two or three genes. In human, the *tweek* homologue is annotated as a single 138 kb gene encoding a very large protein named fsa (Cao et al., 2006; Kuo et al., 2006). Although the predicted amino acid sequence of *Drosophila* Tweek aligns well with its human counterpart over the full length protein (e.g. 30 % identity with mouse Tweek), there are numerous regions that show much higher similarity and identity than the remaining areas (Figure S2). Hence, the sequence of Tweek does not reveal any particular information about its possible function.

To determine the expression pattern of *tweek* we performed *in situ* hybridization to embryos. As shown in Figure 2D, *tweek* is widely expressed but enriched in the brain lobes and in the ventral nerve cord after stage 14 of embryogenesis. We also observe expression in the midgut anlagen. Expression in the CNS becomes stronger in stage 15 embryos. These data are consistent with RT-PCR analyses that reveal expression of human Tweek/Fsa in the brain (McKay et al., 2003). Anti-sense dioxygenin labeled RNA probes complementary to the different 2 *CGs* show identical RNA expression patterns (Figure 2D and Figure S3). Moreover, the gene located 5' of *CG15133* reveals a very different expression pattern than that of the *tweek CG*s (data not shown). Hence, *tweek* encodes a very large transcript that is expressed in the nervous system.

HHMI Author Manuscript HHMI Author Manuscript HHMI Author Manuscript

tweek mutants display defects in neurotransmitter release upon repetitive stimulation

Drosophila mutations that affect synaptic vesicle exocytosis show reduced neurotransmitter release during low frequency stimulation, (e.g. SNAP25, syntaxin, CSP, hip14, cacaphony) whereas mutations that affect endocytosis or recycling (e.g. endophilin, AP180, synaptojanin, eps15, dap160, synapsin) do not affect release under such conditions. Hence to determine if *tweek* affects synaptic transmission we first stimulated motorneurons at low frequency in the presence of 1 or 5 mM Ca^{2+} and recorded excitatory junctional potentials (EJPs). Neither the resting membrane potential, nor the amplitude of the EJPs recorded during low frequency stimulation (<1 Hz) in various *tweek* mutants are different from controls (Figure 3A and Figure S4A, B). These data indicate that *tweek* mutations do not dramatically impair exocytosis under these conditions.

Next we tested the ability of *tweek* mutants to maintain release during intense stimulation. As shown in Figure 3B, EJP amplitudes in *tweek* mutants declined to about 55–60% of the initial response when stimulated at 10 Hz in 5 mM Ca^{2+}. In contrast, controls maintain release at about 90% of the initial response after 10 min at 10 Hz (Figure 3B). The inability of *tweek* mutants to maintain normal levels of transmission during intense activity is consistent with a defect in vesicle trafficking or recycling.

Tweek is required in neurons for proper FM1–43 dye uptake

Synaptic vesicle density in *tweek* mutant PRs is lower than in controls (Figure 1), suggesting a defect to maintain a normal synaptic vesicle pool. To assess if vesicle recycling is affected, we performed live imaging with FM 1–43 dye at third instar NMJs (Ramaswami et al., 1994). In aqueous environments, FM 1–43 is non-fluorescent, but when bound to membranes it increases its fluorescence quantum yield. Hence, newly endocytosed vesicles in the presence of FM 1–43 will be fluorescently labeled, providing a quantitative measure of vesicle uptake (Betz and Bewick, 1992;Verstreken et al., 2007). As shown in Figure 3C and D and Figure S4, when controls, including *tweek* mutants that carry the genomic rescue construct, are stimulated for 1 min with 90 mM KCl or for 10 min with 10 Hz nerve stimulation in the presence of FM 1–43, synapses are brightly labeled, indicating efficient vesicle retrieval from the membrane during stimulation. In contrast, *tweek* mutant synapses are labeled less.

To test if this defect is caused by loss of *tweek* in motor neurons we expressed different RNAi constructs (VDRC) (Dietzl et al., 2007) against *tweek*. RT-PCR and quantitative RT-PCR shows that expression of three RNAi constructs leads to decreased *TWEEK* mRNA levels (Figure S5 and data not shown). We stimulated synapses of animals that express these RNAi constructs in neurons using *nsyb::Gal4* for 1 min in 90 mM KCl and assessed FM 1–43 dye uptake efficiency. As shown in Figure 3E and F, expression of *8060GD (CG15133), 19305GD (CG15134)* or *19306GD (CG15134)* results in a significant reduction of FM 1–43 dye uptake, whereas expression of RNAi constructs that do not significantly affect *tweek* expression show normal uptake. These data indicate that *tweek* acts in the presynaptic neuron and are consistent with an endocytic defect and/or a reduced synaptic vesicle pool.

tweek affects synaptic vesicle density and size

To further explore presynaptic defects in *tweek* mutants we performed TEM at third instar NMJ boutons. As shown in Figure 4, synaptic vesicle number is reduced in *tweek* mutant boutons. While many synaptic features such as mitochondrial number or structure (Figure 4A–C, G), dense body number (T-bars) (Figure 4H–I) dense body morphology (Figure 4 E and F) and the number of docked synaptic vesicles within a 200 nm radius around dense bodies (Figure 4E–F, J) appear normal in *tweek* mutants compared to controls, vesicle counts reveal ~64% less vesicles per unit area (Figure 4A–D, K). *tweek* boutons also contain more large diameter vesicles than controls: the diameter of synaptic vesicles is typically <50 nm in controls (Figure

HHMI Author Manuscript HHMI Author Manuscript HHMI Author Manuscript

4A, L–M), but *tweek* mutants contain numerous vesicles and cisternae that exceed this diameter (Figure 4B–D, L–M). Hence, loss of Tweek, similar to endocytic mutants *AP180/lap*, *dap160*, *eps15*, and *stoned* (Chen et al., 1998;Fergestad et al., 1999;Gonzalez-Gaitan and Jackle, 1997;Stahelin et al., 2003;Stimson et al., 2001;Zhang et al., 1998), leads to reduced vesicle density and causes the formation of larger and more heterogeneously-sized vesicles.

The fusion of large synaptic vesicles should lead to an increased amount of neurotransmitter released per single vesicle fusion event (Zhang et al., 1998). We therefore recorded spontaneous vesicle fusion events (minis) in current clamp mode (miniature excitatory junctional potentials - mEJPs) (Figure 5A) as well as in voltage clamp mode (miniature excitatory junctional currents - mEJCs) (Figure 5B–C, F). As shown in a cumulative probability plot of mEJP amplitudes (Figure 5A) or by calculating the average mEJP (not shown) and mEJC amplitudes (Figure 5B), mini amplitudes in *tweek* mutants are larger compared to controls. In addition, we also find a significant reduction in mini frequency (Figure 5C). These data suggest that single vesicle fusions can elicit larger responses in *tweek* mutants compared to controls. Since GluRIIA and GluRIIC/III immunohistochemical staining of post synaptic glutamate receptors (Marrus et al., 2004; Schuster et al., 1991) do not show differences in receptor cluster size or cluster intensity between *tweek* and controls (GluRIIC/III cluster intensity in control: 100±8.0% and in $tweek^{1}/tweek^{2}$: 88.8±1.5, t-test: p=0.29), synaptic vesicles in *tweek* mutants release abnormally large quantities of neurotransmitters in agreement with an increased vesicle size in the mutants.

EJP amplitudes are similar in controls and *tweek* mutants but mini amplitudes are not. Hence, the number of vesicles released per stimulus (quantal content) is likely altered in *tweek*, possibly as a result of homeostatic regulation (Davis, 2006). To calculate the quantal content we recorded EJC amplitudes in 1 mM Ca^{2+} (Figure 5D–E) and divided the average EJC amplitude by the average mEJC amplitude (quantal amplitude; Figure 5B). Our data indicate that the quantal content in *tweek* is reduced by 31–37% compared to controls (Figure 5G). However, as vesicles in *tweek* are larger, the amount of membrane added per stimulus is comparable or even slightly increased in *tweek* when compared to controls (Figure 5H). Hence, during stimulation, mutants and controls release similar amounts of synaptic vesicle membrane. Since FM1–43 dye uptake is reduced, these data further support a defect in endocytosis or recycling in *tweek* mutants.

Proteins required for proper clathrin coat assembly are decreased at *tweek* NMJs

α-adaptin, AP180/Lap and StonedB are adaptor-like proteins that have been implicated in early steps of vesicle recovery and mutations in the genes that encode these proteins lead to qualitatively similar phenotypes as *tweek* (Fergestad et al., 1999; Gonzalez-Gaitan and Jackle, 1997; Stimson et al., 2001; Zhang et al., 1998). We therefore assessed the levels of these proteins in *tweek* mutant boutons ($tweek^{2}$/ *Df(2L)Exel8036*, $tweek^{1}/tweek^{2}$ and for α-adaptin also $tweek^{2}/tweek^{c01084}$). The levels of these proteins are markedly reduced in *tweek* NMJ boutons (Figure 6A–C and G and data not shown). This decrease is not due to reduced expression levels of these proteins, as Western Blots using whole larval extracts did not show obvious differences between *tweek* and controls (Figure 6I and quantification in the legend).

To assess if *tweek* mutations affect the localization of other endocytic proteins we labeled NMJs with antibodies against Dynamin (van der Bliek and Meyerowitz, 1991), Dap160, Eps15 (Koh et al., 2004; Majumdar et al., 2006; Marie et al., 2004; Roos and Kelly, 1999) and Endophilin (Verstreken et al., 2002). As shown in Figure 6D–F and H, *tweek* does not affect the level or localization of these proteins. In summary, Tweek mediates the normal recruitment, retention and/or stability of several endocytic adaptor-like proteins that are intrinsic components of the clathrin coat.

HHMI Author Manuscript HHMI Author Manuscript HHMI Author Manuscript

$PI(4,5)P_2$ availability is reduced at *tweek* NMJs

Several endocytic adaptors have been shown to interact with phosphorylated inositides (e.g. $PI(4,5)P_2$ - reviewed in (Lemmon, 2003; Wenk and De Camilli, 2004). One possibility therefore is that Tweek affects the levels or distribution of synaptic PIs, thought to be critical for vesicle recycling (Cremona et al., 1999; Di Paolo et al., 2004; Micheva et al., 2001; Verstreken et al., 2003). To estimate the PI levels at *tweek* NMJ boutons we expressed a PI-interacting protein domain fused to EGFP that reports $PI(4,5)P_2$ levels *in vivo* (Jost et al., 1998; Varnai and Balla, 2006).

To visualize $PI(4,5)P_2$ we cloned an EGFP-fused pleckstrin homology (PH) domain of PLCδ1, known to bind $PI(4,5)P_2$ (Varnai and Balla, 1998), in *pUAST* and expressed it using the *UAS-GAL4* system. To test the specificity of this probe, we also expressed a mutant PLCδ-PH^{mut}-EGFP that cannot bind $PI(4,5)P_2$ (Varnai and Balla, 2006). As shown in Figure S6A, the wild type PLCδ-PH-EGFP probe decorates the membrane in salivary gland cells, whereas the mutant PLCδ-PH^{mut}-EGFP is diffusely present in the cytoplasm and concentrates in the nucleus (Figure S6B). Furthermore, in neurons of the larval ventral nerve cord and in the adult brain, PLCδ-PH-EGFP is present in the neuropil synapses (Figure S6C). In contrast, the mutant PLCδ-PH^{mut}-EGFP is diffusely present in the cytoplasm, labeling mostly the cell bodies and less the neuropil (Figure S6D and data not shown). These data indicate that in *Drosophila* the PLCδ-PH-EGFP probe is enriched at synapses (Micheva et al., 2001).

To explore possible changes in levels or distribution of $PI(4,5)P_2$ at the NMJ, we used *elav-Gal4* to express the PLCδ-PH-EGFP probe in the nervous system of *tweek* mutants and wild type controls. In wild type controls the probe is present at synaptic boutons and enriched on their membranes (Figure 7A). We also expressed the probe in *synj* mutants as a positive control to assess the ability of the probe to reveal changes in $PI(4,5)P_2$. Synj is a pre-synaptic phosphoinositide phosphatase, and mouse as well as fly *synj* mutants show an overall increase in the concentration of $PI(4,5)P_2$ (Cremona et al., 1999; Voronov et al., 2008; L.S. and P.D., unpublished results). In agreement with these observations, the signal produced by PLCδ-PH-EGFP at $synj^1$ mutant synapses is increased (Figure 7B and D). In contrast to *synj* and to controls, the levels of PLCδ-PH-EGFP fluorescence expressed using *elav-Gal4* are decreased in *tweek* mutants (Figure 7C and D, Figure S7). This difference is not due to an effect of *tweek* on GFP fluorescence as the levels and localization of untagged GFP, expressed in neurons, is not significantly different in *tweek* versus controls (Figure 7M and N). Hence, these results suggest that Tweek is required to maintain normal levels or availability of $PI(4,5)P_2$ at *Drosophila* NMJs.

To analyze the dynamics of $PI(4,5)P_2$ localization in control and *tweek* mutants during vesicle cycling we performed live imaging of PLCδ-PH-EGFP driven by the strong neuronal *nsyb-Gal4* driver, while stimulating the motor nerve for 100 s at 20 Hz. In controls PLCδ-PH-EGFP distribution during stimulation shows no obvious changes when compared to synapses at rest whereas the PLCδ-PH-EGFP distribution in *tweek* mutants shows obvious differences (Figure 7E–H). Prior to stimulation the distribution of PLCδ-PH-EGFP in controls and *tweek* mutants are similar. Note however that the levels of PLCδ-PH-EGFP are decreased when compared to controls (Figure 7E–H). During stimulation, PLCδ-PH-EGFP redistributes and concentrates in presynaptic clusters in *tweek* mutants, while the mutant PLCvδ-PH^{mut}-EGFP probe does not concentrate in such clusters (Figure 7H, H' and H" and data not shown). These structures in *tweek* mutants often persist for ~100 s after cessation of the stimulation (Figure 7I and J). The clusters may represent lingering endocytic intermediates that still harbor $PI(4,5)P_2$. Hence, the data suggest that Tweek not only affects the basal levels of $PI(4,5)P_2$ but also its synaptic distribution during neuronal activity.

HHMI Author Manuscript HHMI Author Manuscript HHMI Author Manuscript

To test if Tweek affects the availability of other PIs we also expressed 2xFYVE-EGFP, a marker for PI(3)P in the nervous system (Wucherpfennig et al., 2003). PI(3)P is enriched on endosomes but limited amounts may also be present on the plasma membrane. However, the expression of 2xFYVE-EGFP in controls and *tweek* mutants is not significantly different (Figure 7K and L), indicating that *tweek* does not affect the localization or abundance of PI(3)P.

Synaptojanin mutations partially suppress endocytic defects in *tweek*

To provide additional in *vivo* evidence that the availability of $PI(4,5)P_2$ is reduced in *tweek*, we tested vesicle uptake in *tweek* mutants with reduced PI phosphatase activity by removing one copy of *synj*. Removal of a single copy of *synpatojanin* may elevate the reduced $PI(4,5)P_2$ levels observed in *tweek* mutants providing strong genetic evidence for a direct link of Tweek to vesicle recycling and PIPs. To assess endocytosis in these animals, we stimulated synapses for 5 min with KCl in the presence of FM 1–43, and measured labeling intensity. Using this protocol, dye uptake in *synj*/+ heterozygotes and controls is indistinguishable, indicating no dominant effect of the $synj^1$ mutation on endocytosis (Figure 8A, D). Interestingly, *tweek* mutants that lack one copy of *synj* ($tweek^1$ $synj^1$/ $tweek^2$ or $tweek^2$ $synj^1$/ *Df(2L)Exel8036*) take up significantly more dye than *tweek* mutants ($tweek^1$/ $tweek^2$ or $tweek^2$/ *Df(2L)Exel8036*) (Figure 8B–D). However, dye uptake in *tweek* mutants that are heterozygous for *synj* is still less than in controls (*eyFLP; FRT40A*) or in *synj*/+. These data indicate that the levels of $PI(4,5)P_2$ can be genetically manipulated to affect FM 1–43 dye uptake.

We also tested if the removal of one copy of *synj* in *tweek* mutants partially restores α-adaptin levels in boutons. While *tweek* mutants ($tweek^1$/ $tweek^2$, $tweek^2$/ *Df(2L)Exel8036* or $tweek^2$/ $tweek^{c01084}$) show reduced α-adaptin levels in synaptic boutons (Figure 6A and G, and Figure 8F and H), removing one copy of *synj* ($tweek^1$ $synj^1$/ $tweek^2$, $tweek^2$ $synj^1$/ *Df(2L)Exel8036* or $tweek^2$ $synj^1$/ $tweek^{c01084}$) partially restores α-adaptin levels (Figure 8 E–H). Hence, levels of an endocytic adaptor protein in *tweek* mutant NMJ synapses can be restored by decreasing phosphoinositide dephosphorylation activity, consistent with the observation that the availability of phosphorylated inositides is reduced in *tweek* mutants.

Discussion

In an unbiased genetic screen to identify genes that affect neuronal communication we have identified mutants that affect different aspects of synaptic function (Hiesinger et al., 2005; Koh et al., 2004; Verstreken et al., 2003). In the same screen, we also identified *tweek*, which encodes a very large protein without established protein motifs. Interestingly, a *C. elegans tweek* homologue *lpd-3* which encodes the carboxyterminal end of Tweek, but is most likely part of a much larger gene (including Y47G6A.23 and Y47G6A.29), was previously identified in an RNAi screen for lipid storage defects (McKay et al., 2003). However, the molecular nature underlying the RNAi phenotype in worms has not been investigated. Our data indicate that *tweek* plays a role in synaptic vesicle recycling likely by regulating PI-lipid signaling at the synapse.

The Tweek protein is unusually large as it encodes a protein of 5,076 amino acids. Interestingly, Tweek does not contain any known motifs, and hence cloning of the gene did not reveal any hints about its potential function or localization. Note that the three CGs that form the *tweek* transcript are also found clustered in other species. These *tweek* homologues have most likely been wrongly annotated in almost all species (except human) as separate genes. No full length cDNA has been reported in any species and when expression patterns are available of portions of the *tweek* homologs, they are localized in the nervous system and fat tissue (Chintapalli et al., 2007; Manak et al., 2006; McKay et al., 2003). In flies, the *TWEEK* RNA transcript is also

HHMI Author Manuscript HHMI Author Manuscript HHMI Author Manuscript

expressed in the CNS, but localization of the protein could not be established as we were unable to raise an antibody upon injection of various antigens in 10 animals. Similarly, localization of the protein using a mCherry-tagged genomic construct that can rescue the *tweek* mutations failed, even when we tried to enhance signal using antibodies against the tag (data not shown). Taken together these data suggest that the protein derived from the *tweek* locus is not abundant and this may explain why it has not been identified previously through biochemical approaches.

tweek mutants harbor the hallmarks of mutants that affect endocytosis. Electrophysiological analyses show that *tweek* mutants fail to maintain neurotransmitter release during intense stimulation and internalize less FM 1–43 dye, indicating a smaller vesicle pool. They also display reduced synaptic vesicle numbers and aberrantly large vesicles. We used Synaptophluorin (Poskanzer et al., 2003) to further test membrane recycling following stimulation (0.2 s at 50 Hz), but observed only a slightly slower and statistically insignificant decay in fluorescence quenching in *tweek* mutants compared to controls. While these data suggest that part of the recycling defect in *tweek* mutants may occur after newly endocytosed vesicles are acidified, we also did not observe a difference in Synaptophluorin fluorescence decay in *dap160* endocytic mutants when compared to controls when stimulated using the same paradigm (Supplemental figure 8). These data suggest that Synaptophluorin may not be able to detect the defects in membrane recycling in these 'endocytic' mutants.

While some of the phenotypes we observe in *tweek* mutants may be recapitulated in other fly mutants (Daniels et al., 2006; Daniels et al., 2004), the *tweek* mutants are phenotypically much more similar to mutants that affect endocytosis. Indeed, *stoned*, *AP180*, *dap160*, and *eps15* mutants all exhibit reduced vesicle numbers (Fergestad et al., 1999; Ferguson et al., 2007; Koh et al., 2004; Majumdar et al., 2006; Marie et al., 2004; Nonet et al., 1999; Stimson et al., 2001; Zhang et al., 1998). These phenotypes combined with the aberrant localization of endocytic adaptor proteins in *tweek* mutants is consistent with the hypothesis that Tweek at least in part affects vesicle recycling early, when adaptor proteins are recruited to the plasma membrane, and this is bolstered by the dominant genetic interaction with *synj*. However, we cannot exclude additional roles for the protein at later steps of the vesicle cycle.

Both synaptic vesicle exocytosis and endocytosis are critically dependent on PIs present at synaptic membranes (Di Paolo et al., 2004; Schiavo et al., 1996; Verstreken et al., 2003). PI(4,5)P_2 in the plasma membrane is thought to be a major anchor point for endocytic adaptor proteins that link clathrin to this membrane (Cremona et al., 1999; Gaidarov et al., 1996). Reduced availability of PI(4,5)P_2 in *tweek* mutants may lead to reduced coat nucleation at the synapse and therefore provides a rationale for the mislocalization of endocytic adaptor proteins in the mutants. While a biochemical link between Tweek, phosphoinositide availability and adaptor localization awaits further investigation, our model is consistent with the observation that increasing the PI(4,5)P_2 levels in *tweek* mutants, by reducing *synj* expression, partially restores the localization of the AP2 adaptor. Note that not all PI(4,5)P_2 interacting proteins are destabilized at *tweek* mutant synapses. For example Dynamin binds PI(4,5)P_2, yet, it seems to be localized similarly in *tweek* and controls. Furthermore, the levels of Synaptotagmin, a synaptic vesicle protein known to interact with PI(4,5)P_2, appears similar in controls and *tweek* mutants (data not shown). We surmise that while PI binding may be mediating the function of these proteins (Achiriloaie et al., 1999; Bai et al., 2004; Zoncu et al., 2007), they may require less PI(4,5)P_2 than adaptor proteins.

Although a large body of evidence demonstrates a role for PI(4,5)P_2 in various cellular processes (Hassan et al., 1998; Horn, 2005; York, 2006), *tweek* mutant cells do not show signs of major cellular dysfunction beyond a defect to maintain synaptic transmission, indicating that the effect of *tweek* loss-of-function in neurons is rather specific to synaptic vesicle recycling. We and others have observed a similar remarkably specific phenotype in *synj*

HHMI Author Manuscript HHMI Author Manuscript HHMI Author Manuscript

mutants (Cremona et al., 1999; Harris et al., 2000; Van Epps et al., 2004; Verstreken et al., 2003). Although *synj* mutants lead to an increase in phosphorylated PIs, defects at the NMJ appear to be specific to synaptic vesicle endocytosis. Hence, specific factors locally regulate the availability of specific PI lipids, even within the synapse. As a result, PI phosphatases, kinases and proteins like Tweek that may control PI availability must play important roles during vesicle recycling.

Methods

Genetics and Molecular Biology

Throughout the paper, control animals were isogenized *y w; P{y$^+$, ry$^+$}25F P{neoFRT}40A* unless otherwise indicated and *tweek$^{1\ or\ 2}$* mutants were (*y w P{ey-FLP.N}2; tweek^1 P{y$^+$, ry$^+$}25F P{neoFRT}40A* and *y w P{ey-FLP.N}2; tweek^2 P{y$^+$, ry$^+$}25F P{neoFRT}40A*. Additional details on *tweek* alleles and identification of the *tweek* gene as well as generation of transgenic animals appear in the Supplemental Methods

Immunohistochemistry and Western Blotting

Labeling was performed following standard protocols and fluorescent images (including EGFP) were captured using a Zeiss 510 confocal microscope and imported in Amira 2.2 to adjust their brightness and contrast and then imported in Photoshop 7.0 to assemble them in figures.

Samples for Western Blots were prepared by crushing third instar larvae in modified HL-3 with 0.4% Triton-X-100 and proteinase inhibitors on ice, and then boiling them in sample buffer for 5 min. Western Blots were run and quantified according to standard protocols.

Antibodies and concentrations for immunohistochemistry/Western Blotting: α-adaptin (Gonzalez-Gaitan and Jackle, 1997) 1:500/1:5000; Dynamin (Upstate) 1:200/0.125μg/ml; Eps15 (Koh et al., 2007) 1:5000/1:10000; Endophilin (Verstreken et al., 2002) 1:200/1:5000; Lap (AP180) (Zhang et al., 1998) 1:150/1:2500; Dap160 (Roos and Kelly, 1999) 1:500/1:5000; StonedB (Phillips et al., 2000) 1:200/1:5000. Antibodies for immunohistochemistry: DLG (mouse; 4F3) (Parnas et al., 2001) 1:50; DLG (rabbit) (Kwang Choi, BCM) 1:500; HRP (Jackson Labs), 1:500; GluRIIA (mouse; 8B4) 1:50 (Schuster et al., 1991) and GLURIII/IIC 1:500 (Marrus et al., 2004). Cy3 (Jackson Labs) or Alexa 488 (Invitrogen) conjugated antibodies were used at 1:250. HRP conjugated antibodies (Jackson Labs) were used at 1:2500.

Labeling intensity of endocytic markers was quantified as described (Koh et al., 2004). Briefly, mutant and control samples were labeled together and imaged using identical settings. Pixel intensities inside the boutonic volumes, circumscribed by an independent marker were calculated using Amira 2.2. For quantification of endocytic markers we used DLG labeling as an independent outline of the boutonic volume and subtracted background labeling in the muscle.

For each lipid-GFP probe at least 3 controls and 3 mutant animals were labeled together with a synaptic marker (anti-HRP). GFP fluorescence of controls and mutants was imaged using identical settings, and using the synaptic marker as an outline of the synapse, we measured absolute GFP fluorescence intensity and normalized this to control values.

Electrophysiology and FM 1–43 dye uptake and live imaging

ERGs and current clamp (CC) recordings were performed as described (Verstreken et al., 2003; Verstreken et al., 2002). Two electrode voltage clamp (TEVC) recordings were made in modified HL-3 [(in mM) NaCl 110; KCl 5; $NaHCO_3$ 10; HEPES 5; Sucrose 30; Threalose 5;

HHMI Author Manuscript

HHMI Author Manuscript

HHMI Author Manuscript

$MgCl_2$ 10; pH 7.2; $CaCl_2$ as indicated in the text; for minis, we added 5 μM TTX. Resting membrane potentials were between −55 and −65 mV and were clamped at −65 mV. Voltage errors were <1.5 mV for 100 nA EJCs, input resistances were ≥ 4 MΩ and data was filtered at 1 kHz.

FM 1–43 dye uptake experiments were performed as described in the text and images were captured with a Zeiss MRm or on a Nikon Digital Sight DS2Mb-Wc camera using a 40x Zeiss or Nikon water immersion lens (NA 0.8) and analyzed and quantified as described (Verstreken et al., 2007).

Live imaging of PLCδ-PH-EGFP was performed as described in the supplemental methods

Transmission Electron Microscopy

TEM of PRs was performed as described in (Hiesinger et al., 2005) and TEM of NMJ boutons was performed as described (Verstreken et al., 2003). Data was analyzed using Image-J.

Supplementary Material

Refer to Web version on PubMed Central for supplementary material.

Acknowledgements

We are grateful to the Bloomington stock center, the Developmental studies hybridoma bank, VDRC, Kwang Choi, Aaron Di Antonio, Barry Dickson, Bruce Edgar, Marcos Gonzalez-Gaitán, Leonard Kelly, Jeanette Kunz, Cahir O'Kane, and Bing Zhang for reagents. We thank Yuchun He for injections, Shinya Yamamoto, Karen Schulze, Elaine Seto, Nikolaos Giagtzoglou, Hiroshi Tsuda, Gilbert Di Paolo, Jeanette Kunz and members of the Bellen, Verstreken and De Camilli labs for comments. PV was supported by a R.L. Kirchstein NRS award, a Marie Curie Excellence Grant (MEXT-CT-2006-042267), the Research Fund K.U.Leuven, FWO grant G.0747.09 and VIB, CVL was supported by an NRS award and PDC and HJB are HHMI investigators.

References

Achiriloaie M, Barylko B, Albanesi JP. Essential role of the dynamin pleckstrin homology domain in receptor-mediated endocytosis. Mol Cell Biol 1999;19:1410–1415. [PubMed: 9891074]

Babcock MC, Stowers RS, Leither J, Goodman CS, Pallanck LJ. A genetic screen for synaptic transmission mutants mapping to the right arm of chromosome 3 in Drosophila. Genetics 2003;165:171–183. [PubMed: 14504225]

Bai J, Tucker WC, Chapman ER. PIP2 increases the speed of response of synaptotagmin and steers its membrane-penetration activity toward the plasma membrane. Nat Struct Mol Biol 2004;11:36–44. [PubMed: 14718921]

Bellen HJ, Levis RW, Liao G, He Y, Carlson JW, Tsang G, Evans-Holm M, Hiesinger PR, Schulze KL, Rubin GM, et al. The BDGP gene disruption project: single transposon insertions associated with 40% of Drosophila genes. Genetics 2004;167:761–781. [PubMed: 15238527]

Betz WJ, Bewick GS. Optical analysis of synaptic vesicle recycling at the frog neuromuscular junction. Science 1992;255:200–203. [PubMed: 1553547]

Cao YW, Jiang CL, Jiang T. Molecular cloning and preliminary analysis of a fragile site associated gene. Biomed Environ Sci 2006;19:392–398. [PubMed: 17190194]

Chen H, Fre S, Slepnev VI, Capua MR, Takei K, Butler MH, Di Fiore PP, De Camilli P. Epsin is an EH-domain-binding protein implicated in clathrin-mediated endocytosis. Nature 1998;394:793–797. [PubMed: 9723620]

Chintapalli VR, Wang J, Dow JA. Using FlyAtlas to identify better Drosophila melanogaster models of human disease. Nat Genet 2007;39:715–720. [PubMed: 17534367]

Cremona O, Di Paolo G, Wenk MR, Luthi A, Kim WT, Takei K, Daniell L, Nemoto Y, Shears SB, Flavell RA, et al. Essential role of phosphoinositide metabolism in synaptic vesicle recycling. Cell 1999;99:179–188. [PubMed: 10535736]

HHMI Author Manuscript HHMI Author Manuscript HHMI Author Manuscript

Daniels RW, Collins CA, Chen K, Gelfand MV, Featherstone DE, DiAntonio A. A single vesicular glutamate transporter is sufficient to fill a synaptic vesicle. Neuron 2006;49:11–16. [PubMed: 16387635]

Daniels RW, Collins CA, Gelfand MV, Dant J, Brooks ES, Krantz DE, DiAntonio A. Increased expression of the Drosophila vesicular glutamate transporter leads to excess glutamate release and a compensatory decrease in quantal content. J Neurosci 2004;24:10466–10474. [PubMed: 15548661]

Davis GW. Homeostatic control of neural activity: from phenomenology to molecular design. Annu Rev Neurosci 2006;29:307–323. [PubMed: 16776588]

Davis ME, Patrick RL. Diacylglycerol-induced stimulation of neurotransmitter release from rat brain striatal synaptosomes. J Neurochem 1990;54:662–668. [PubMed: 2299360]

Di Paolo G, Pellegrini L, Letinic K, Cestra G, Zoncu R, Voronov S, Chang S, Guo J, Wenk MR, De Camilli P. Recruitment and regulation of phosphatidylinositol phosphate kinase type 1 gamma by the FERM domain of talin. Nature 2002;420:85–89. [PubMed: 12422219]

Di Paolo G, Moskowitz HS, Gipson K, Wenk MR, Voronov S, Obayashi M, Flavell R, Fitzsimonds RM, Ryan TA, De Camilli P. Impaired PtdIns(4,5)P2 synthesis in nerve terminals produces defects in synaptic vesicle trafficking. Nature 2004;431:415–422. [PubMed: 15386003]

Dietzl G, Chen D, Schnorrer F, Su KC, Barinova Y, Fellner M, Gasser B, Kinsey K, Oppel S, Scheiblauer S, et al. A genome-wide transgenic RNAi library for conditional gene inactivation in Drosophila. Nature 2007;448:151–156. [PubMed: 17625558]

Fabian-Fine R, Verstreken P, Hiesinger PR, Horne JA, Kostyleva R, Zhou Y, Bellen HJ, Meinertzhagen IA. Endophilin promotes a late step in endocytosis at glial invaginations in Drosophila photoreceptor terminals. J Neurosci 2003;23:10732–10744. [PubMed: 14627659]

Fergestad T, Davis WS, Broadie K. The stoned proteins regulate synaptic vesicle recycling in the presynaptic terminal. J Neurosci 1999;19:5847–5860. [PubMed: 10407025]

Ferguson SM, Brasnjo G, Hayashi M, Wolfel M, Collesi C, Giovedi S, Raimondi A, Gong LW, Ariel P, Paradise S, et al. A selective activity-dependent requirement for dynamin 1 in synaptic vesicle endocytosis. Science 2007;316:570–574. [PubMed: 17463283]

Gaidarov I, Chen Q, Falck JR, Reddy KK, Keen JH. A functional phosphatidylinositol 3,4,5-trisphosphate/phosphoinositide binding domain in the clathrin adaptor AP-2 alpha subunit. Implications for the endocytic pathway. J Biol Chem 1996;271:20922–20929. [PubMed: 8702850]

Gong LW, Di Paolo G, Diaz E, Cestra G, Diaz ME, Lindau M, De Camilli P, Toomre D. Phosphatidylinositol phosphate kinase type I gamma regulates dynamics of large dense-core vesicle fusion. Proc Natl Acad Sci U S A 2005;102:5204–5209. [PubMed: 15793002]

Gonzalez-Gaitan M, Jackle H. Role of Drosophila alpha-adaptin in presynaptic vesicle recycling. Cell 1997;88:767–776. [PubMed: 9118220]

Golub T, Caroni P. PI(4,5)P2-dependent microdomain assemblies capture microtubules to promote and control leading edge motility. The Journal of cell biology 2005;169:151–165. [PubMed: 15809307]

Harris TW, Hartwieg E, Horvitz HR, Jorgensen EM. Mutations in synaptojanin disrupt synaptic vesicle recycling. J Cell Biol 2000;150:589–600. [PubMed: 10931870]

Hassan BA, Prokopenko SN, Breuer S, Zhang B, Paululat A, Bellen HJ. skittles, a Drosophila phosphatidylinositol 4-phosphate 5-kinase, is required for cell viability, germline development and bristle morphology, but not for neurotransmitter release. Genetics 1998;150:1527–1537. [PubMed: 9832529]

Haucke V. Where proteins and lipids meet: membrane trafficking on the move. Dev Cell 2003;4:153–157. [PubMed: 12586059]

Hiesinger PR, Fayyazuddin A, Mehta SQ, Rosenmund T, Schulze KL, Zhai RG, Verstreken P, Cao Y, Zhou Y, Kunz J, Bellen HJ. The v-ATPase V0 subunit a1 is required for a late step in synaptic vesicle exocytosis in Drosophila. Cell 2005;121:607–620. [PubMed: 15907473]

Horn R. Electrifying phosphatases. Sci STKE 2005;2005:pe50. [PubMed: 16249403]

Jost M, Simpson F, Kavran JM, Lemmon MA, Schmid SL. Phosphatidylinositol-4,5-bisphosphate is required for endocytic coated vesicle formation. Curr Biol 1998;8:1399–1402. [PubMed: 9889104]

Jung N, Haucke V. Clathrin-mediated endocytosis at synapses. Traffic 2007;8:1129–1136. [PubMed: 17547698]

HHMI Author Manuscript HHMI Author Manuscript HHMI Author Manuscript

Kasprowicz J, Kuenen S, Miskiewicz K, Habets RL, Smitz L, Verstreken P. Inactivation of clathrin heavy chain inhibits synaptic recycling but allows bulk membrane uptake. J Cell Biol 2008;182:1007–1016. [PubMed: 18762582]

Koh TW, Verstreken P, Bellen HJ. Dap160/intersectin acts as a stabilizing scaffold required for synaptic development and vesicle endocytosis. Neuron 2004;43:193–205. [PubMed: 15260956]

Kuo MT, Wei Y, Yang X, Tatebe S, Liu J, Troncoso P, Sahin A, Ro JY, Hamilton SR, Savaraj N. Association of fragile site-associated (FSA) gene expression with epithelial differentiation and tumor development. Biochem Biophys Res Commun 2006;340:887–893. [PubMed: 16386706]

Lemmon MA. Phosphoinositide recognition domains. Traffic 2003;4:201–213. [PubMed: 12694559]

Majumdar A, Ramagiri S, Rikhy R. Drosophila homologue of Eps15 is essential for synaptic vesicle recycling. Exp Cell Res 2006;312:2288–2298. [PubMed: 16709407]

Manak JR, Dike S, Sementchenko V, Kapranov P, Biemar F, Long J, Cheng J, Bell I, Ghosh S, Piccolboni A, Gingeras TR. Biological function of unannotated transcription during the early development of Drosophila melanogaster. Nat Genet 2006;38:1151–1158. [PubMed: 16951679]

Mani M, Lee SY, Lucast L, Cremona O, Di Paolo G, De Camilli P, Ryan TA. The dual phosphatase activity of synaptojanin1 is required for both efficient synaptic vesicle endocytosis and reavailability at nerve terminals. Neuron 2007;56:1004–1018. [PubMed: 18093523]

Marie B, Sweeney ST, Poskanzer KE, Roos J, Kelly RB, Davis GW. Dap160/intersectin scaffolds the periactive zone to achieve high-fidelity endocytosis and normal synaptic growth. Neuron 2004;43:207–219. [PubMed: 15260957]

Marrus SB, Portman SL, Allen MJ, Moffat KG, DiAntonio A. Differential localization of glutamate receptor subunits at the Drosophila neuromuscular junction. J Neurosci 2004;24:1406–1415. [PubMed: 14960613]

Martin TF. Phosphoinositide lipids as signaling molecules: common themes for signal transduction, cytoskeletal regulation, and membrane trafficking. Annu Rev Cell Dev Biol 1998;14:231–264. [PubMed: 9891784]

McKay RM, McKay JP, Avery L, Graff JM. C elegans: a model for exploring the genetics of fat storage. Dev Cell 2003;4:131–142. [PubMed: 12530969]

Micheva KD, Holz RW, Smith SJ. Regulation of presynaptic phosphatidylinositol 4,5-biphosphate by neuronal activity. J Cell Biol 2001;154:355–368. [PubMed: 11470824]

Milosevic I, Sorensen JB, Lang T, Krauss M, Nagy G, Haucke V, Jahn R, Neher E. Plasmalemmal phosphatidylinositol-4,5-bisphosphate level regulates the releasable vesicle pool size in chromaffin cells. J Neurosci 2005;25:2557–2565. [PubMed: 15758165]

Newsome TP, Asling B, Dickson BJ. Analysis of Drosophila photoreceptor axon guidance in eye-specific mosaics. Development 2000;127:851–860. [PubMed: 10648243]

Nonet ML, Holgado AM, Brewer F, Serpe CJ, Norbeck BA, Holleran J, Wei L, Hartwieg E, Jorgensen EM, Alfonso A. UNC-11, a Caenorhabditis elegans AP180 homologue, regulates the size and protein composition of synaptic vesicles. Mol Biol Cell 1999;10:2343–2360. [PubMed: 10397769]

Parks AL, Cook KR, Belvin M, Dompe NA, Fawcett R, Huppert K, Tan LR, Winter CG, Bogart KP, Deal JE, et al. Systematic generation of high-resolution deletion coverage of the Drosophila melanogaster genome. Nat Genet 2004;36:288–292. [PubMed: 14981519]

Parnas D, Haghighi AP, Fetter RD, Kim SW, Goodman CS. Regulation of postsynaptic structure and protein localization by the Rho-type guanine nucleotide exchange factor dPix. Neuron 2001;32:415–424. [PubMed: 11709153]

Phillips AM, Smith M, Ramaswami M, Kelly LE. The products of the Drosophila stoned locus interact with synaptic vesicles via synaptotagmin. J Neurosci 2000;20:8254–8261. [PubMed: 11069931]

Poskanzer KE, Marek KW, Sweeney ST, Davis GW. Synaptotagmin I is necessary for compensatory synaptic vesicle endocytosis in vivo. Nature 2003;426:559–563. [PubMed: 14634669]

Ramaswami M, Krishnan KS, Kelly RB. Intermediates in synaptic vesicle recycling revealed by optical imaging of Drosophila neuromuscular junctions. Neuron 1994;13:363–375. [PubMed: 8060617]

Rhee JS, Betz A, Pyott S, Reim K, Varoqueaux F, Augustin I, Hesse D, Sudhof TC, Takahashi M, Rosenmund C, Brose N. Beta phorbol ester- and diacylglycerol-induced augmentation of transmitter release is mediated by Munc13s and not by PKCs. Cell 2002;108:121–133. [PubMed: 11792326]

HHMI Author Manuscript HHMI Author Manuscript HHMI Author Manuscript

Roos J, Kelly RB. The endocytic machinery in nerve terminals surrounds sites of exocytosis. Curr Biol 1999;9:1411–1414. [PubMed: 10607569]

Schiavo G, Gu QM, Prestwich GD, Sollner TH, Rothman JE. Calcium-dependent switching of the specificity of phosphoinositide binding to synaptotagmin. Proc Natl Acad Sci U S A 1996;93:13327–13332. [PubMed: 8917590]

Schuske KR, Richmond JE, Matthies DS, Davis WS, Runz S, Rube DA, van der Bliek AM, Jorgensen EM. Endophilin is required for synaptic vesicle endocytosis by localizing synaptojanin. Neuron 2003;40:749–762. [PubMed: 14622579]

Schuster CM, Ultsch A, Schloss P, Cox JA, Schmitt B, Betz H. Molecular cloning of an invertebrate glutamate receptor subunit expressed in Drosophila muscle. Science 1991;254:112–114. [PubMed: 1681587]

Sladeczek F. Putative role of inositol phospholipid metabolism in neurons. Biochimie 1987;69:287–296. [PubMed: 2820514]

Stahelin RV, Long F, Peter BJ, Murray D, De Camilli P, McMahon HT, Cho W. Contrasting membrane interaction mechanisms of AP180 N-terminal homology (ANTH) and epsin N-terminal homology (ENTH) domains. J Biol Chem 2003;278:28993–28999. [PubMed: 12740367]

Stimson DT, Estes PS, Rao S, Krishnan KS, Kelly LE, Ramaswami M. Drosophila stoned proteins regulate the rate and fidelity of synaptic vesicle internalization. J Neurosci 2001;21:3034–3044. [PubMed: 11312288]

Stowers RS, Schwarz TL. A genetic method for generating Drosophila eyes composed exclusively of mitotic clones of a single genotype. Genetics 1999;152:1631–1939. [PubMed: 10430588]

van der Bliek AM, Meyerowitz EM. Dynamin-like protein encoded by the Drosophila shibire gene associated with vesicular traffic. Nature 1991;351:411–414. [PubMed: 1674590]

Van Epps HA, Hayashi M, Lucast L, Stearns GW, Hurley JB, De Camilli P, Brockerhoff SE. The zebrafish nrc mutant reveals a role for the polyphosphoinositide phosphatase synaptojanin 1 in cone photoreceptor ribbon anchoring. J Neurosci 2004;24:8641–8650. [PubMed: 15470129]

Varnai P, Balla T. Visualization of phosphoinositides that bind pleckstrin homology domains: calcium- and agonist-induced dynamic changes and relationship to myo-[3H]inositol-labeled phosphoinositide pools. J Cell Biol 1998;143:501–510. [PubMed: 9786958]

Varnai P, Balla T. Live cell imaging of phosphoinositide dynamics with fluorescent protein domains. Biochim Biophys Acta 2006;1761:957–967. [PubMed: 16702024]

Venken KJ, He Y, Hoskins RA, Bellen HJ. P[acman]: a BAC transgenic platform for targeted insertion of large DNA fragments in D. melanogaster. Science 2006;314:1747–1751. [PubMed: 17138868]

Verstreken P, Kjaerulff O, Lloyd TE, Atkinson R, Zhou Y, Meinertzhagen IA, Bellen HJ. Endophilin mutations block clathrin-mediated endocytosis but not neurotransmitter release. Cell 2002;109:101–112. [PubMed: 11955450]

Verstreken P, Koh TW, Schulze KL, Zhai RG, Hiesinger PR, Zhou Y, Mehta SQ, Cao Y, Roos J, Bellen HJ. Synaptojanin is recruited by endophilin to promote synaptic vesicle uncoating. Neuron 2003;40:733–748. [PubMed: 14622578]

Verstreken P, Ohyama T, Bellen HJ. FM 1–43 labeling at the Drosophila neuromuscular junction. Methods in Molecular Biology 2007;440:349–369. [PubMed: 18369958]

Vicinanza M, D'Angelo G, Di Campli A, De Matteis MA. Function and dysfunction of the PI system in membrane trafficking. EMBO J 2008;27:2457–2470. [PubMed: 18784754]

Voronov SV, Frere SG, Giovedi S, Pollina EA, Borel C, Zhang H, Schmidt C, Akeson EC, Wenk MR, Cimasoni L, et al. Synaptojanin 1-linked phosphoinositide dyshomeostasis and cognitive deficits in mouse models of Down's syndrome. Proc Natl Acad Sci U S A 2008;105:9415–9420. [PubMed: 18591654]

Wenk MR, De Camilli P. Protein-lipid interactions and phosphoinositide metabolism in membrane traffic: insights from vesicle recycling in nerve terminals. Proc Natl Acad Sci U S A 2004;101:8262–8269. [PubMed: 15146067]

Wucherpfennig T, Wilsch-Brauninger M, Gonzalez-Gaitan M. Role of Drosophila Rab5 during endosomal trafficking at the synapse and evoked neurotransmitter release. J Cell Biol 2003;161:609–624. [PubMed: 12743108]

HHMI Author Manuscript

York JD. Regulation of nuclear processes by inositol polyphosphates. Biochim Biophys Acta 2006;1761:552–559. [PubMed: 16781889]

Zhai RG, Hiesinger PR, Koh TW, Verstreken P, Schulze KL, Cao Y, Jafar-Nejad H, Norga KK, Pan H, Bayat V, et al. Mapping Drosophila mutations with molecularly defined P element insertions. Proc Natl Acad Sci U S A 2003;100:10860–10865. [PubMed: 12960394]

Zhang B, Koh YH, Beckstead RB, Budnik V, Ganetzky B, Bellen HJ. Synaptic vesicle size and number are regulated by a clathrin adaptor protein required for endocytosis. Neuron 1998;21:1465–1475. [PubMed: 9883738]

Zoncu R, Perera RM, Sebastian R, Nakatsu F, Chen H, Balla T, Ayala G, Toomre D, De Camilli PV. Loss of endocytic clathrin-coated pits upon acute depletion of phosphatidylinositol 4,5-bisphosphate. Proc Natl Acad Sci U S A 2007;104:3793–3798. [PubMed: 17360432]

HHMI Author Manuscript
HHMI Author Manuscript
HHMI Author Manuscript

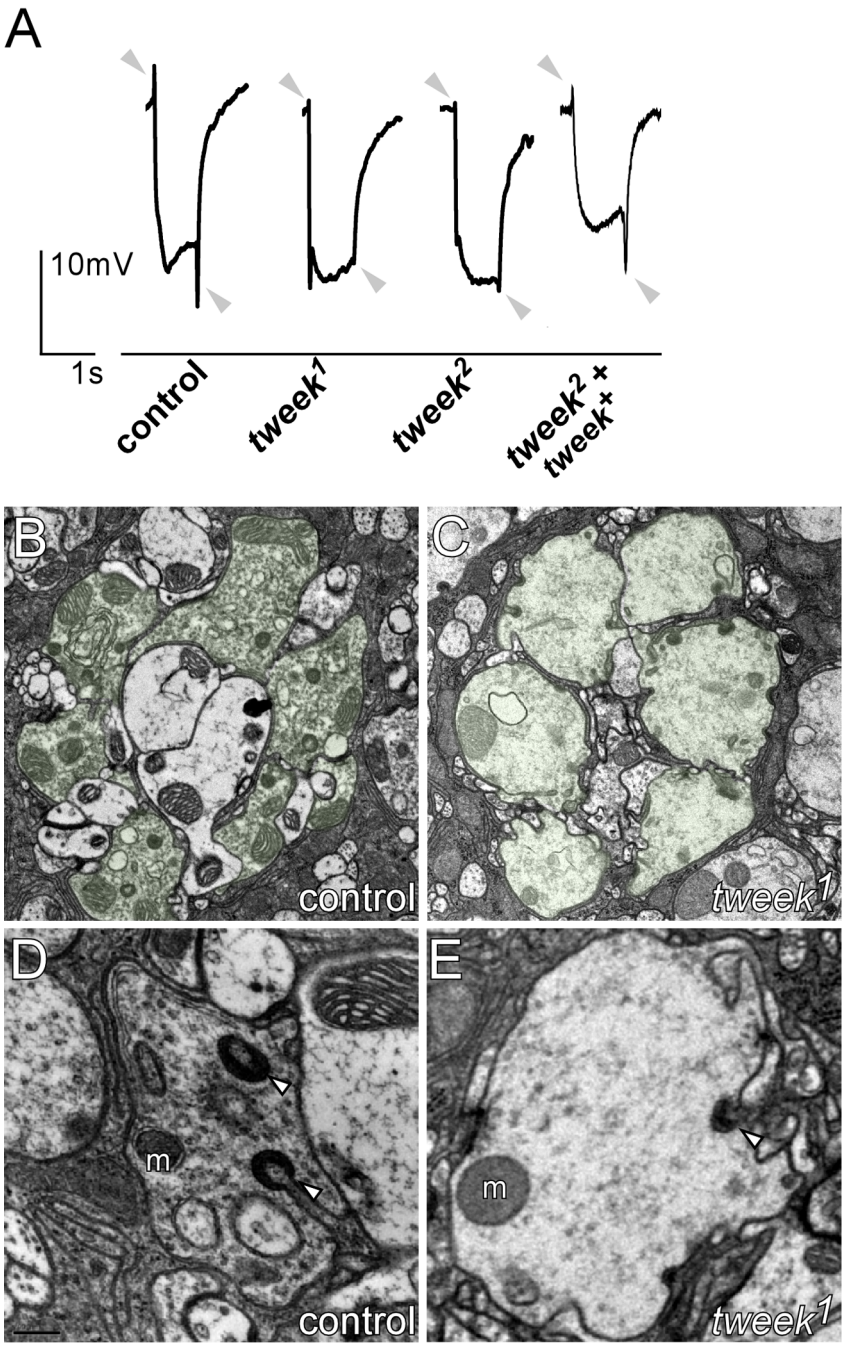

Figure 1. *tweek* mutant photoreceptors show synaptic defects

(A) Electroretinograms of controls (*yw eyFLP; P{y*$^{+}$*} FRT40A / l(2)cl-2L P{w*$^{+}$*} FRT40A*), *tweek* mutants (*yw eyFLP; tweek*$^{1\ or\ 2}$ *P{y*$^{+}$*} FRT40A / l(2)cl-2L P{w*$^{+}$*} FRT40A*) and rescued *tweek* animals (*yw eyFLP; tweek* ^{2} *P{y*$^{+}$*} FRT40A; tweek*$^{+}$*(HB69)* / +). The positions of 'on' and 'off' transients (or lack thereof) are indicated by grey arrows.

(B–C) Electron microscopy of control (*yw eyFLP; P{y*$^{+}$*} FRT40A / l(2)cl-2L P{w*$^{+}$*} FRT40A*) and *tweek*^{1} mutant (*yw eyFLP; tweek*^{1} *P{y*$^{+}$*} FRT40A / l(2)cl-2L P{w*$^{+}$*} FRT40A*) lamina cartridges. PR terminals of one cartridge are artificially labeled in green.

(D–E) Electron microscopy images of single PR terminals of control (C) and *tweek*^{1} mutant (D) animals. Capitate projections (arrowhead) and mitochondria (m) are indicated.

HHMI Author Manuscript
HHMI Author Manuscript
HHMI Author Manuscript

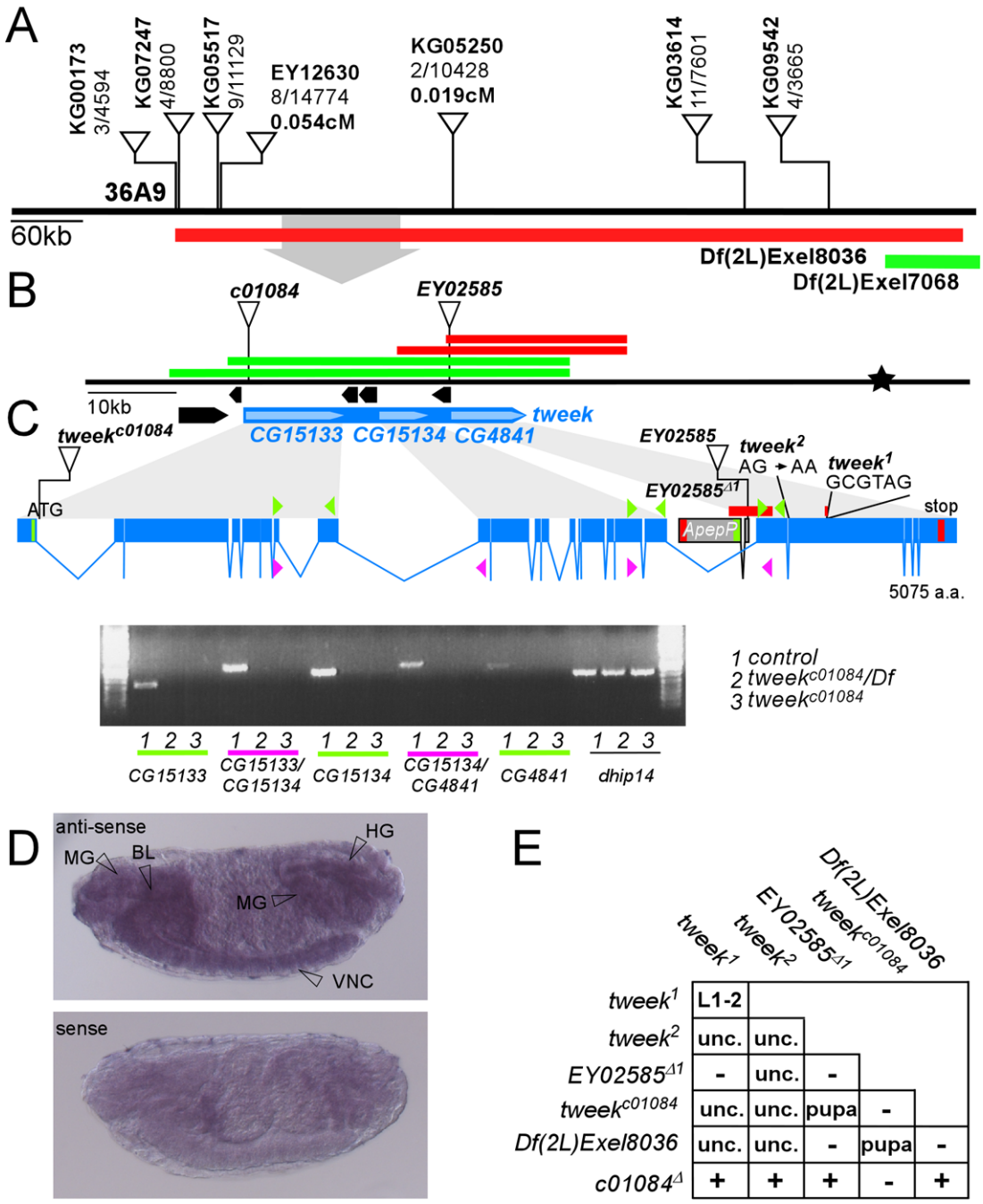

Figure 2. Characterization of *tweek* mutants

(A) *P*-element mapping. *P*-elements used for mapping: numbers separated by a "/" indicate the number of recombinants out of flies scored. Recombination distance in cM for two nearby *P*-elements is indicated. The cytological interval and the Exelixis deficiencies that complement (Green) or not (Red) are shown. The area magnified in (B) is shown by a grey arrow

(B) The mapping location of *tweek* (Blue) based on recombination data (Star). *CG15133*, *CG15134* and *CG4841* correspond to the *tweek* gene. *EY02528*, as well as *c01084* fail to complement the *tweek*$^{1 \text{ and } 2}$ alleles. The regions cloned in P[acman] to create rescue constructs are indicated: red constructs do not rescue the *tweek* alleles while the green constructs do rescue the *tweek* alleles.

HHMI Author Manuscript HHMI Author Manuscript HHMI Author Manuscript

(C) Intron-exon structure of *tweek* and RT-PCR analysis. Start codons are marked in green and stop codons in red. The *P*-element excision $EY02585^{\Delta 1}$ and the molecular nature of both *tweek* alleles are indicated. $tweek^{1}$ harbors a 74 bp deletion (red) and a 6 bp insertion (indicated) and $tweek^{2}$ harbors a splice acceptor mutation before exon 20. RT-PCR on *yw eyFLP; FRT40A*^{iso} control, $tweek^{c01084}$ and $tweek^{c01084}/Df(2L)Exel8036$ using the primers shown in Supplemental Table 1. (D) *In situ* hybridization of dioxygenin labeled RNA to whole stage 15 embryos using a *CG4841* probe revealing labeling in the mid gut (MG), hind gut (HG), brain lobe (BL) and ventral nerve cord (VNC). An independent probe against *CG15134* shows an identical labeling pattern (see Figure S3) while sense probes do not show specific labeling. (E) Lethal stage of *tweek* mutant combinations. L1-2: animals do not survive beyond the first or second instar larval stage. Pupa or Unc: most animals die during the pharate adult (late pupal) stage. However, very few (<1/2,000) manage to eclose but are severely uncoordinated. −: failure to complement, +: complement.

HHMI Author Manuscript
HHMI Author Manuscript
HHMI Author Manuscript

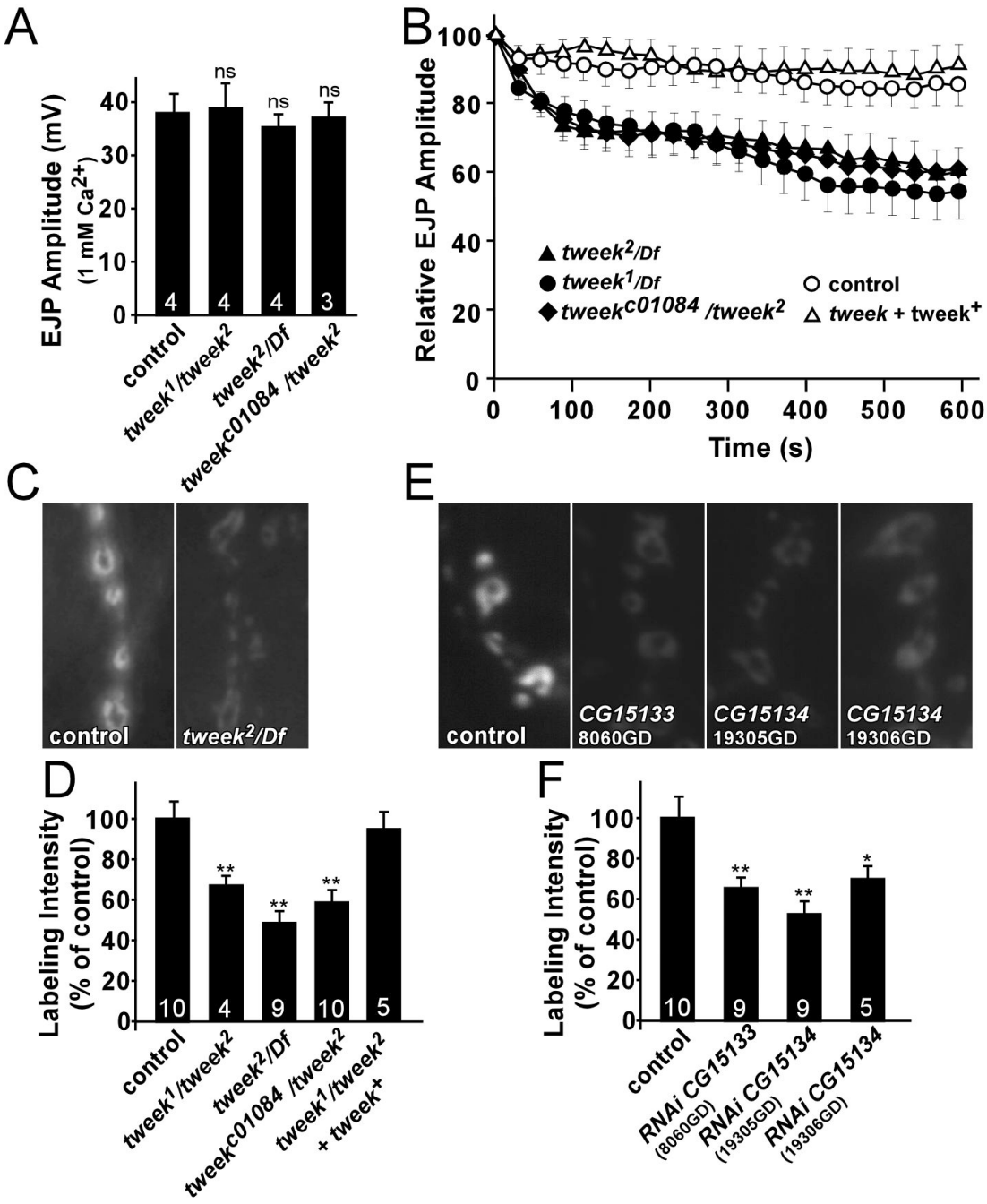

Figure 3. Synaptic vesicle endocytosis is impaired in *tweek* mutants

(A) Average EJP amplitude recorded in 1 mM Ca^{2+} in controls, *tweek*^{1}/*tweek*^{2}, *tweek*$_{2}$/*Df* and *tweek*^{c01084}/*tweek*^{2}. Recordings were performed for 1 min at 1 Hz and 60 EJP amplitudes were averaged per recording. Under these conditions, there are no exocytic defects in *tweek* mutants.

(B) Average EJP amplitudes recorded at 10 Hz for 10 min in 5 mM external Ca^{2+} in controls, *tweek*^{1}/*Df*, *tweek*^{2}/*Df*, *tweek*^{c01084}/*tweek*^{2} and *tweek*^{1}/*tweek*^{2}; *tweek*$^{+}$(+*HB69*) rescued animals. Average EJP amplitudes (binned per 30 s) are normalized to the initial response (an average of the first 5 EJPs).

(C–F) FM 1–43 dye uptake in controls (*yw; P{y*$^{+}$*} FRT40A*) (C,D) or (*UAS-DCR2 / w*^{1118}*; nSyb-Gal4 /* $^{+}$) (E,F), *tweek*^{1}/*tweek*^{2} mutants (*yw eyFLP; tweek*^{1} *P{y*$^{+}$*} FRT40A / tweek*^{2} *P*

HHMI Author Manuscript HHMI Author Manuscript HHMI Author Manuscript

{y+} FRT40A), *tweek2/Df* mutants (*eyFLP; tweek2 P{y+} FRT40A / Df(2L)Exel8036*), *tweekc01084 / tweek2* mutants (*eyFLP; tweek2 P{y+} FRT40A / tweekc01084*), *tweek1/tweek2* mutants with a rescue construct (*yw eyFLP; tweek1 P{y+} FRT40A / tweek2 P{y+} FRT40A; tweek+(HB69)/+*) (C,D) and flies that express RNAi directed against *TWEEK* (*UAS-DCR2 / w1118; 8060GD / +; nSyb-Gal4 / +* or *UAS-DCR2 / w1118; nSyb-Gal4 / 19305GD or 19306GD*) (E,F). Preparations were incubated in 4 μM dye and were stimulated with 1 min of 90 mM KCl to label the exo-endo cycling pool.

* *p<0.05*; ** *p<0.01* (t-test), ns: not significant, Error bars: SEM, *n* (the number of animals tested) is indicated in the bars.

HHMI Author Manuscript
HHMI Author Manuscript
HHMI Author Manuscript

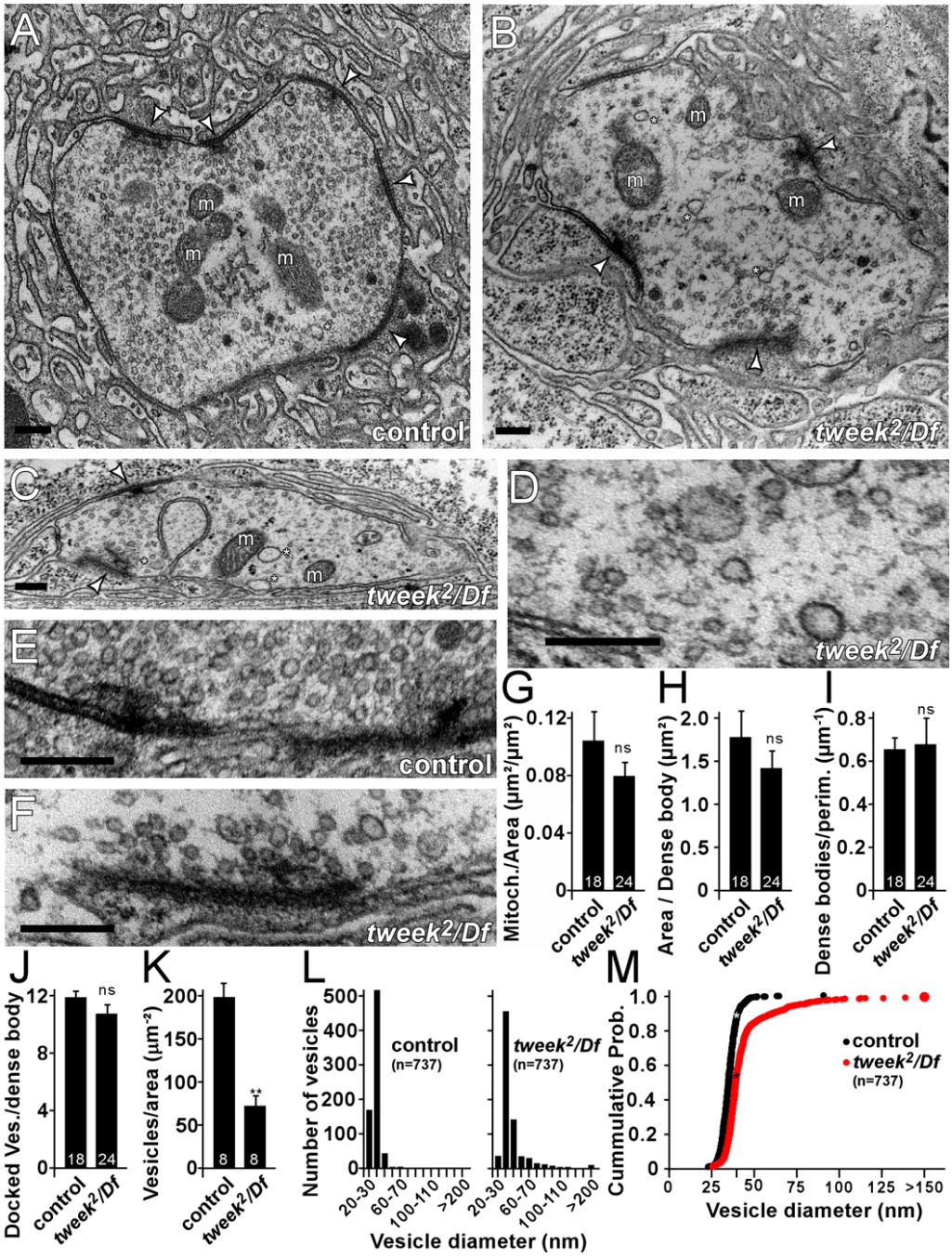

Figure 4. Vesicle size and number are altered in *tweek* mutants

(A–F) Ultrastructure of control (*yw; P{y⁺} FRT40A*) (A, E) and *tweek²/Df* (*yw eyFLP; tweek² P{y⁺} FRT40A / Df(2L)Exel8036*) mutants (B–D, F) NMJ boutons (A–D) and dense bodies (E–F). Note the reduced synaptic vesicle density and the heterogeneity in synaptic vesicle size (asterisks) in the mutants compared to the control. Dense bodies (arrowheads) and mitochondria (m) are marked. Scale bars are 200 nm.

(G–K) Quantification of ultrastructural features: mitochondrial density (G), boutonic area per dense body (H), dense bodies per perimeter bouton (I), number of docked vesicles synaptic in a 200 nm radius around the dense body (J) and synaptic vesicle density (K). ** *p<0.01* (t-test),

ns, not significant; Error bars: SEM, The number of analyzed sections is indicated in the bars and images were acquired from 8 boutons in 5 different animals.
(L–M) Histograms of synaptic vesicle diameter in controls and *tweek*^{2}/ *Df* and cumulative histogram of synaptic vesicle diameters indicating larger vesicles in *tweek* mutants. 737 vesicle diameters were measured for each genotype.

HHMI Author Manuscript HHMI Author Manuscript HHMI Author Manuscript

HHMI Author Manuscript
HHMI Author Manuscript
HHMI Author Manuscript

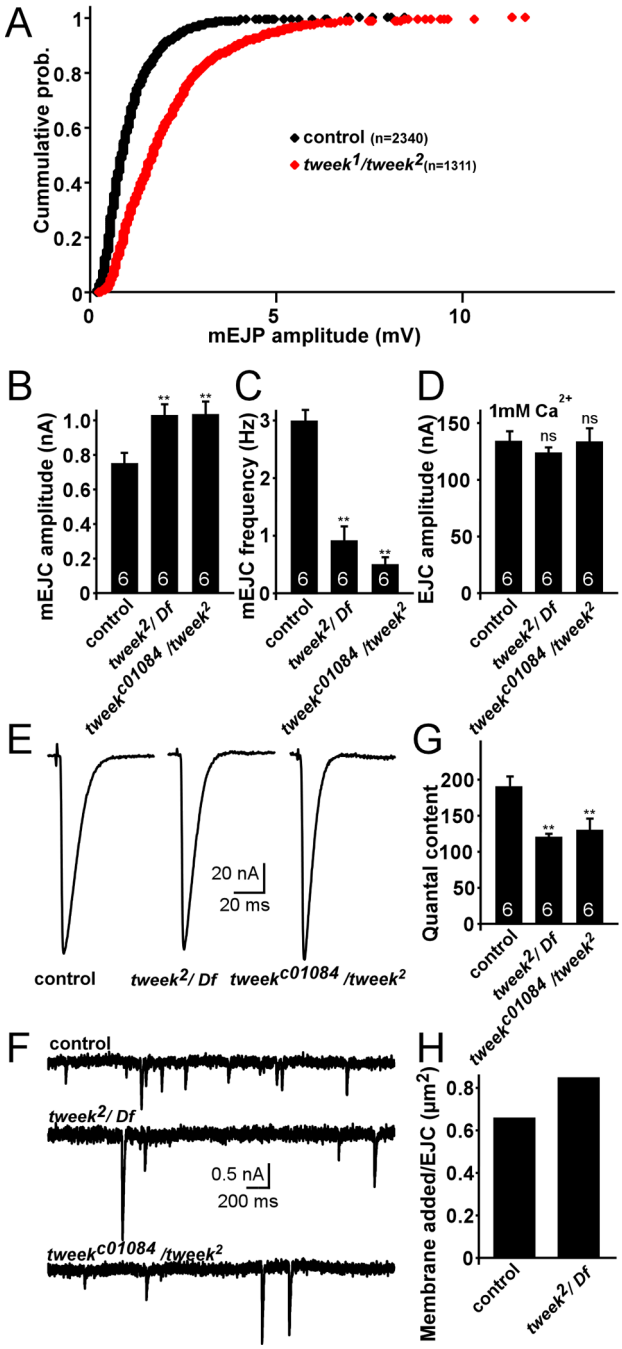

Figure 5. Quantal size is increased in *tweek* mutants

(A) Cumulative histogram of mEJPs measured from controls (black: *yw; P{y+} FRT40A*) and *tweek*^{1}/*tweek*^{2} (red: *yw eyFLP; tweek*^{1} *P{y+} FRT40A / tweek*^{1} *P{y+} FRT40A*) animals. Note the rightward shift in *tweek* mutants signifying larger mEJP amplitudes.

(B–C) Average mEJC amplitude (B) and frequency (C) in controls and *tweek* mutants (*tweek*^{2}/*Df* :*yw eyFLP; tweek*^{2} *P{y+} FRT40A / Df(2L)Exel8036* and *tweek*^{c01084}/ *tweek*^{2}: *yw eyFLP; tweek*^{2} *P{y+} FRT40A / tweek*^{c01084}).

(D) Average EJC amplitude in controls and *tweek* mutants recorded in 1 mM extracellular Ca^{2+}.

HHMI Author Manuscript

HHMI Author Manuscript

HHMI Author Manuscript

(E–F) Sample EJC (E) and mEJC (F) traces recorded from controls and *tweek* mutants. Recordings were performed for 1 min at 0.1 Hz and all EJC amplitudes were averaged per recording.

(G) Junctional quantal content at 1 mM Ca^{2+} calculated by dividing the average EJC amplitude by the average mEJC amplitude. ** $p<0.01$ (t-test), Error bars: SEM, *n* (the number of animals tested) is indicated in the bars.

(H) Estimation of vesicular membrane added per stimulus in 1 mM extracellular Ca^{2+} calculated by multiplying the quantal content (control: 189 quanta; *tweek*^{2}/*Df*: 120 quanta) by the average vesicle surface area based on TEM in Figure 4 (control: vesicle radius 16.7 nm; *tweek*^{2}/*Df*: vesicle radius 23.8 nm).

HHMI Author Manuscript
HHMI Author Manuscript
HHMI Author Manuscript

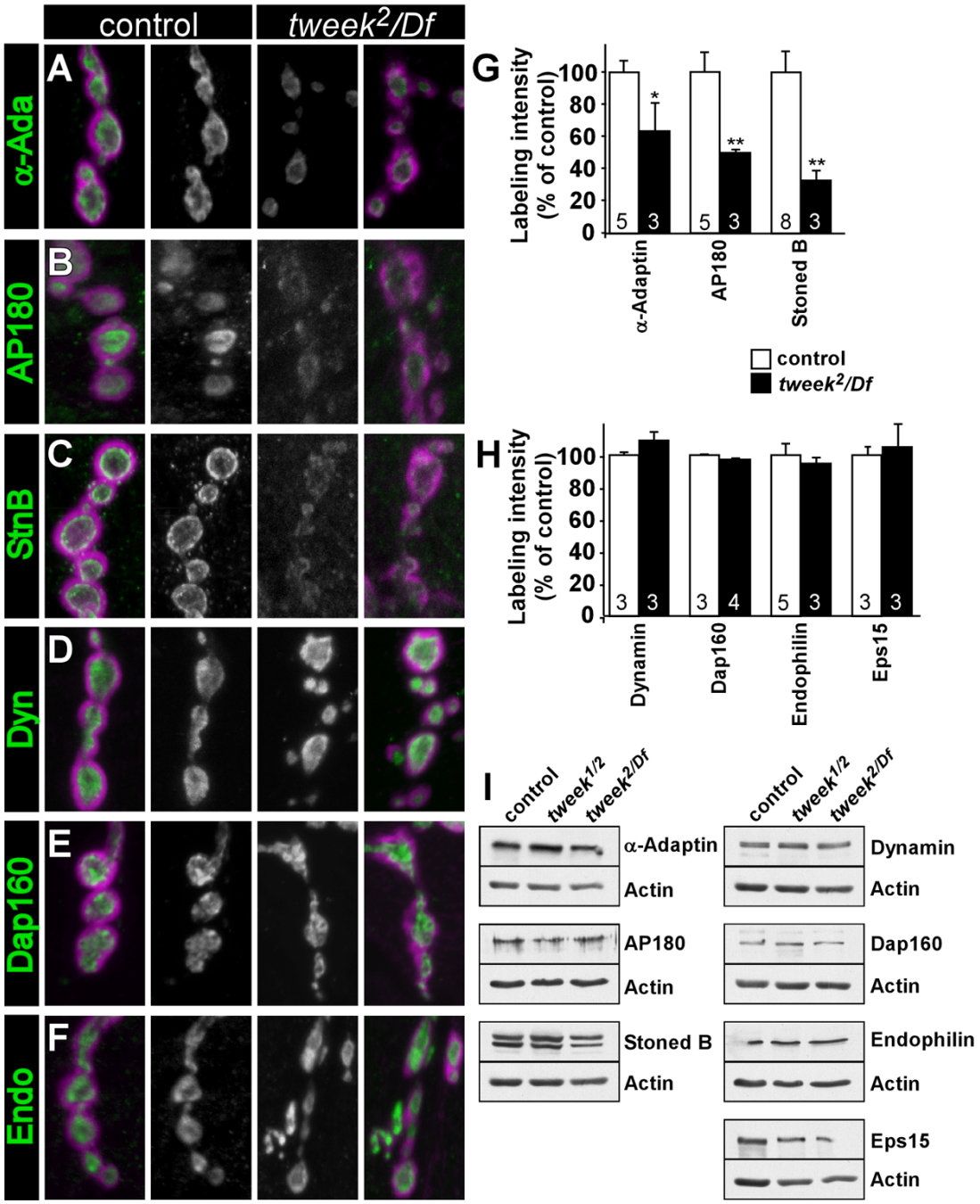

Figure 6. Endocytic adaptor proteins are destabilized at *tweek* mutant boutons

(A–F) Confocal images showing labeling of control (*yw; P{y*$^{+}$*} FRT40A*) (left) and *tweek*^{2}*/Df* (*yw eyFLP; tweek*^{2} *P{y*$^{+}$*} FRT40A / Df(2L)Exel8036*) (light) larval filets with α-adaptin (A), AP180/Lap (B), StonedB (C), Dynamin (D), Dap160/Intersectin (E) Endophilin (F) (green) and DLG/PSD-95 (magenta). Green channel labeling for control and *tweek*^{2}*/Df* is shown in the middle (gray scale).

(G–H) Quantification of boutonic labeling intensity (inside the respective DLG circumscribed areas) for markers shown in (A–F) and for Eps15. Data for *tweek*^{1}*/tweek*^{2} mutants (*yw eyFLP; tweek*^{1} *P{y*$^{+}$*} FRT40A / tweek*^{2} *P{y*$^{+}$*} FRT40A*) is very similar to *tweek*^{2}*/Df* mutants (not

shown). * $p<0.05$, ** $p<0.01$ (t-test), Error bars: SEM, *n* (the number on animals labeled) is indicated in the bars.

(I) Western Blots of larval extracts of controls, *tweek*^{1}/*tweek*^{2} and *tweek*^{2}/*Df* using antibodies against the endocytic proteins tested in (A–H). Protein loading amounts were tested with anti-actin antibodies. Quantification of 3 independent Westerns normalized to actin loading control (values relative to control levels): α-adaptin: control: 100.0±12.7%; *tweek*^{1}/*tweek*^{2}: 95.8 ±19.1%; *tweek*^{2}/*Df(2L)Exel8036*: 86.4±20.3%; *p*:ns. Lap/AP180: control: 100.0±6.4%; *tweek*^{1}/*tweek*^{2}: 94.2±8.9%; *tweek*^{2}/*Df(2L)Exel8036*: 82.3±21.2%; *p*:ns. stonedB: control: 100.0±23.0%; *tweek*^{1}/*tweek*^{2}: 87.4±15.3%; *tweek2/Df(2L)Exel8036*: 81.5±2.4%; *p*:ns.

HHMI Author Manuscript HHMI Author Manuscript HHMI Author Manuscript

HHMI Author Manuscript
HHMI Author Manuscript
HHMI Author Manuscript

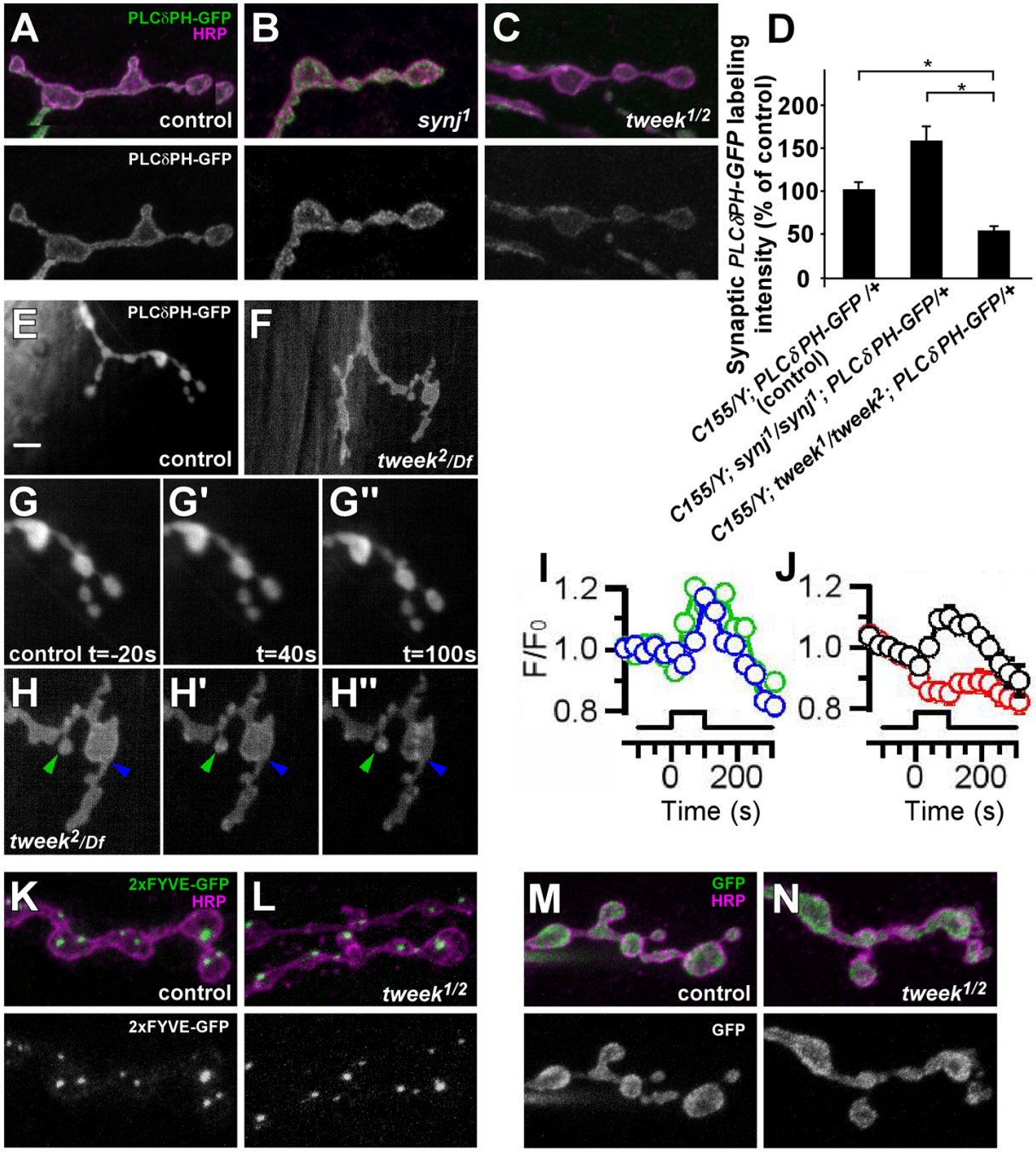

Figure 7. Synaptic PI(4,5)P_2 levels are reduced in *tweek* mutants

(A–C) Neuronal PI(4,5)P_2 levels in boutons of control (*elav-GAL4/Y; UAS-PLCδ-PH-EGFP / +*), *synj*^{1} (*elav-GAL4/Y; FRT42D synj*^{1}*; UAS-PLCδ-PH-EGFP / +*) and *tweek*^{1}*/ tweek*^{2} (*elav-GAL4/Y; tweek*^{1} *P{y*$^+$*} FRT40A / tweek*^{2} *P{y*$^+$*} FRT40A; UAS-PLCδ-PH-EGFP / +*) third instar filets were visualized by a PLCδ-PH-EGFP probe (green). Neuronal membranes were counterstained with anti-HRP (magenta). Green channel is separately shown on the bottom. Note increased EGFP levels in *synj1* mutants and decreased EGFP levels in *tweek* mutants.

(D) Quantification of PLCδ-PH-EGFP intensity shown in (A–C) inside the volume demarcated by anti-HRP labeling in the indicated genotypes. * $p<0.05$ (t-test)

HHMI Author Manuscript HHMI Author Manuscript HHMI Author Manuscript

(E–H) Live imaging of PLCδ-PH-EGFP localization before (E, F, G and H) and after 40s (G', H') or 100s (G", H") of 20 Hz stimulation of (E and G–G") control (*yw /w; FRT40A /+; UAS-PLCδ-PH-EGFP, nsyb-Gal4/+*) and (F and H–H") *tweek*^{2}*/Df* (*yw /w; tweek*^{2} *FRT40A / Df(2L) Exel8036; UAS-PLCδ-PH-EGFP, nsyb-Gal4/+*) third instar NMJs. GFP imaging was performed with a CCD camera and G and H are magnifications of E and F respectively. Controls never show PLCδ-PH-EGFP clusters (n= 7 animals) whereas numerous PLCδ-PH-EGFP clusters (green and blue arrowhead) appear in *tweek* mutants during stimulation. Such clusters are not observed using the PLCδ-PH^{MUT}-EGFP, indicating specificity. Scale bar: 5 μm.
(I–J) Quantification of the fluorescence of PLCδ-PH-EGFP clusters during stimulation (start at t=0, marked by the bar). (I) Green and blue traces show the normalized fluorescence of individual clusters indicated in H–H", showing that some clusters form early in the stimulus (green) and others form later (blue). Note also that clusters remain for an extended period of time (>100 s) following stimulation before they dissapear (J) Black trace shows the average ± SEM for all clusters formed in the *tweek*^{2}*/Df* experiments (23 clusters, 4 animals). The red trace shows the corresponding change in fluorescence in the remainder of the terminal of *tweek*^{2}*/Df*, and this trace appears very similar to the one measured from control boutons where also no clusters were observed (G–G").
(K–L) Neuronal PI(3)P levels in boutons of control (*elav-GAL4/Y; UAS-2xFYVE-EGFP* / +) or *tweek*^{1}*/tweek*^{2} mutants (*elav-GAL4/Y; tweek*^{2} *UAS-2xFYVE-EGFP / tweek*^{1} *P{y*$^{+}$*} FRT40A*) third instar filets were visualized with a 2xFYVE-EGFP probe (green). Neuronal membranes were counterstained with anti-HRP (magenta). Green channel is separately shown on the bottom.
(M–N) Neuronal GFP levels in boutons of control (*elav-GAL4/Y; UAS-GFP* / +) or *tweek*^{1}*/ tweek*^{2} mutant (*elav-GAL4/Y; tweek*^{2} *UAS-GFP / tweek*^{1} *P{y*$^{+}$*} FRT40A*) third instar filets (green). Neuronal membranes were counterstained with anti-HRP (magenta). Green channel is separately shown on the bottom.

HHMI Author Manuscript
HHMI Author Manuscript
HHMI Author Manuscript

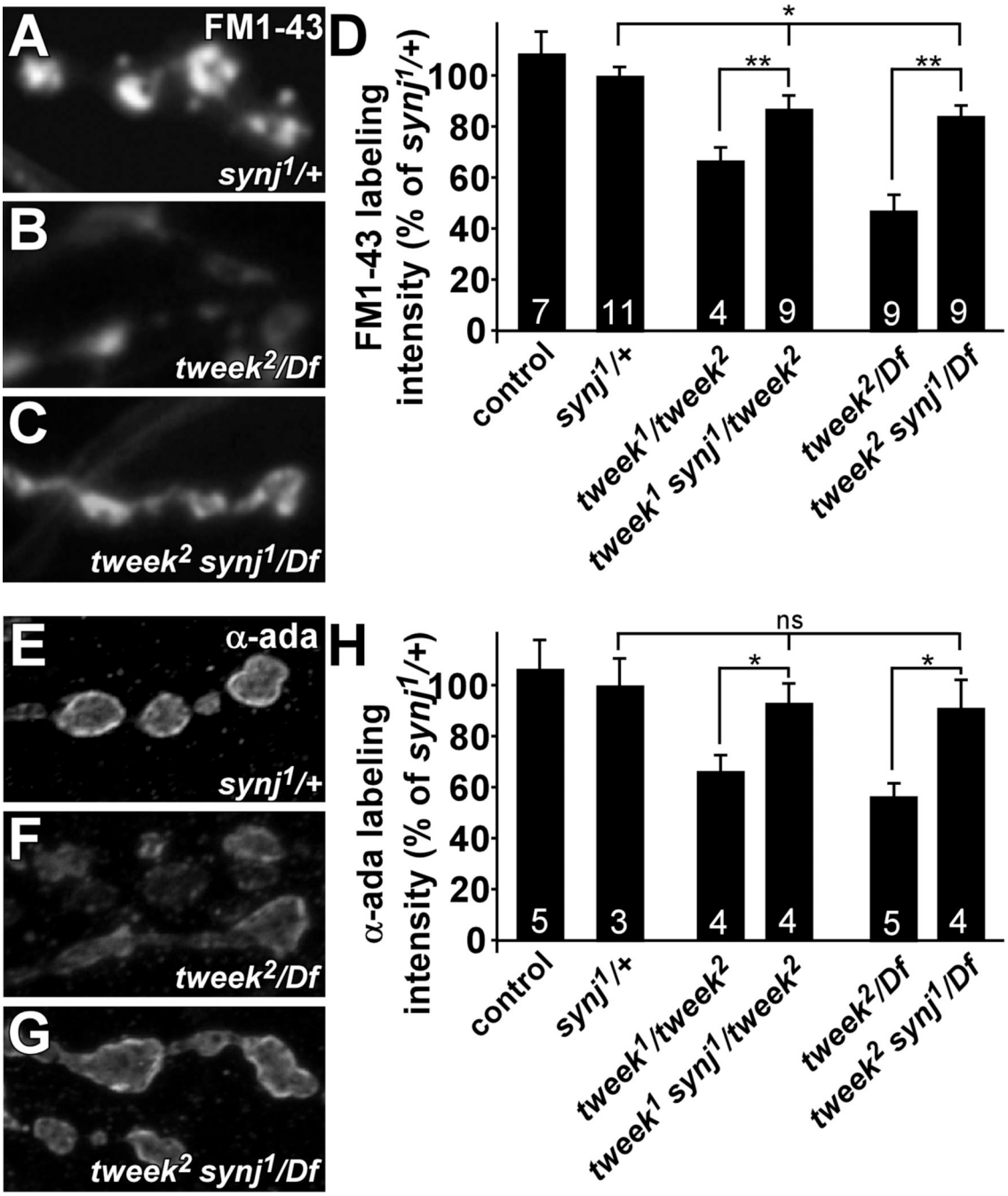

Figure 8. Removal of a single mutant copy of *synaptojanin* suppresses endocytic defects in *tweek*

(A–D) FM 1–43 dye uptake experiment on *synj*^{1}/+x controls (*yw ey-FLP*; *FRT42D synj*^{1} / *FRT42D*), *tweek*^{2}*/Df* mutants (*yw eyFLP; tweek*^{2} *P{y*$^{+}$*} FRT40A / Df(2L)Exel8036*) and *tweek*^{2}*/Df* mutants that lack one functional copy of the *synj* gene (*yw ey-FLP / yw*; *tweek* ^{2} *synj*^{1} */ Df(2L)Exel8036*). Preparations were stimulated in 90 mM KCl for 5 min, washed and imaged (A–C) and labeling intensity quantified (D). Dye uptake in *synj1/+* and *yw eyFLP; FRT40A* controls is indistinguishable (shown in D). Note the increased FM 1–43 dye uptake in *tweek* mutants with reduced *synj* function compared to *tweek* mutants. To measure PI(4,5) P_2 levels in *synj*^{1} and *synj*^{1}/+ animals we expressed the PLCδ-PH-EGFP probe and measured boutonic fluorescence relative to controls: 100±12% for controls (*elav-GAL4/Y; P{w*$^{+}$*UAS-*

HHMI Author Manuscript

HHMI Author Manuscript

HHMI Author Manuscript

PLCδ-PH-EGFP} / +); 157±20% $p<0.05$ for $synj^{1}$ (*elav-GAL4/Y; P{neoFRT}42D* $synj^{1}$*; P* $\{w^{+}$*UAS-PLCδ-PH-EGFP}* / +); 117±8% $p<0.1$ for $synj^{1}$/+ (*elav-GAL4/Y; P{neoFRT}42D* $synj^{1}$/+; $P\{w^{+}$*UAS-PLCδ-PH-EGFP}* / +).

(E–H) α-adaptin labeling in $synj^{1}$/+ controls, $tweek^{2}$*/Df* mutants and $tweek^{2}$*/Df* mutants that lack one functional copy of the *synj* gene ($tweek^{2}$ $synj^{1}$*/Df*). (H) Quantification of α-adaptin labeling intensity. α-adaptin labeling in $synj^{1}$/+ and *yw eyFLP; FRT40A* controls is indistinguishable (shown in D). Note the increased α-adaptin labeling in *tweek* mutants with reduced *synj* function compared to *tweek* mutants. * $p<0.05$, ** $p<0.01$ (t-test), Error bars: SEM, *n* (the number on animals labeled) is indicated in the bars.